iScience

CellPress
OPEN ACCESS

Article

Mice lacking DKK1 in T cells exhibit high bone mass and are protected from estrogen-deficiency-induced bone loss

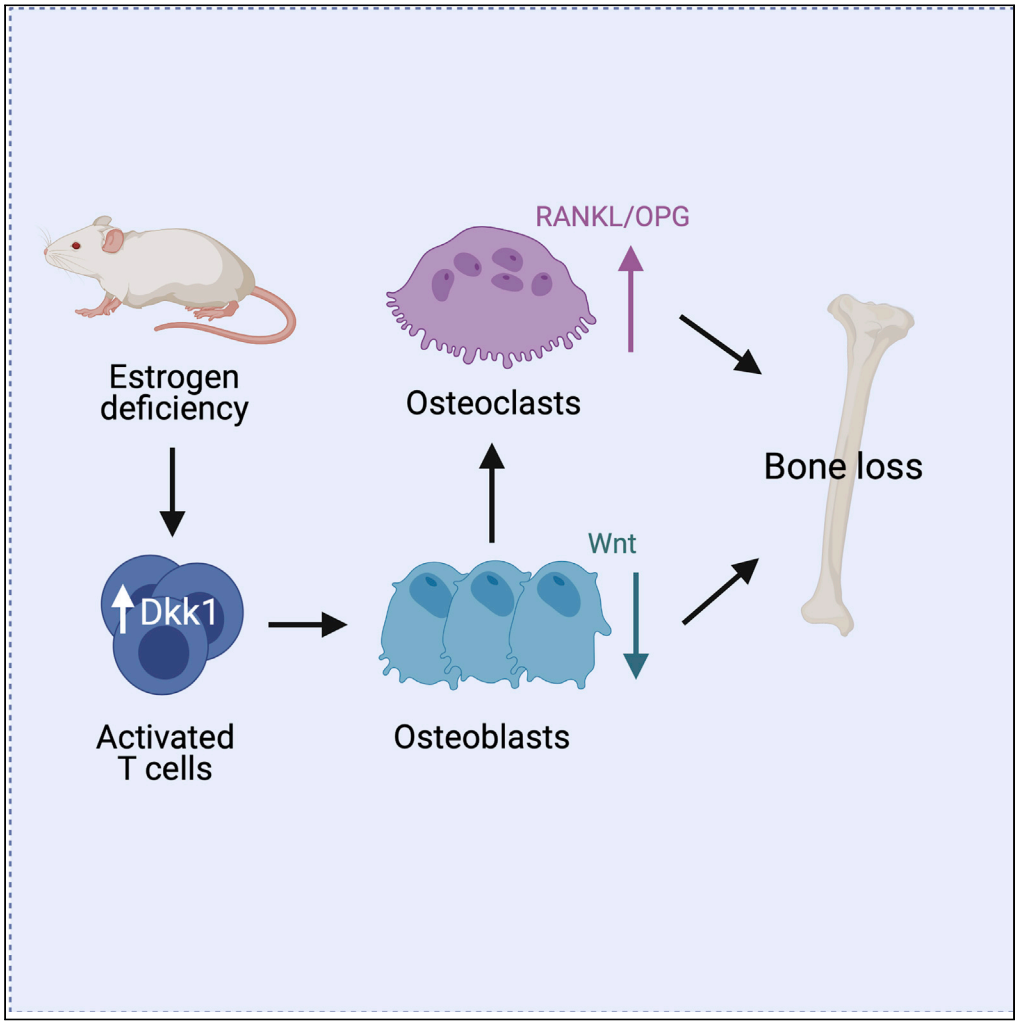

Juliane Lehmann, Sylvia Thiele, Ulrike Baschant, Tilman D. Rachner, Christof Niehrs, Lorenz C. Hofbauer, Martina Rauner

martina.rauner@ukdd.de

HIGHLIGHTS

Lack of DKK1 in T cells leads to high bone mass due to increased bone formation

Activated T cells deficient of DKK1 suppress osteoblast marker expression

Mice with T cells deficient of DKK1 are protected from ovariectomy-induced bone loss

Lehmann et al., iScience *24*, 102224
March 19, 2021
https://doi.org/10.1016/j.isci.2021.102224

iScience

CellPress
OPEN ACCESS

Article

Mice lacking DKK1 in T cells exhibit high bone mass and are protected from estrogen-deficiency-induced bone loss

Juliane Lehmann,[1,2] Sylvia Thiele,[1,2] Ulrike Baschant,[1,2] Tilman D. Rachner,[1,2] Christof Niehrs,[4,5] Lorenz C. Hofbauer,[1,3] and Martina Rauner[1,2,6,*]

SUMMARY

The Wnt inhibitor Dickkopf-1 (DKK1) is a negative regulator of bone formation and bone mass and is dysregulated in various bone diseases. How DKK1 contributes to postmenopausal osteoporosis, however, remains poorly understood. Here, we show that mice lacking DKK1 in T cells are protected from ovariectomy-induced bone loss. Ovariectomy activated CD4+ and CD8+ T cells and increased their production of DKK1. Co-culture of activated T cells with osteoblasts inhibited Wnt signaling in osteoblasts, leading to impaired differentiation. Importantly, DKK1 expression in T cells also controlled physiological bone remodeling. T-cell-deficient *Dkk1* knock-out mice had a higher bone mass with an increased bone formation rate and decreased numbers of osteoclasts compared with controls, a phenotype that was rescued by adoptive transfer of wild-type T cells. Thus, these findings highlight that T cells control bone remodeling in health and disease via their expression of DKK1.

INTRODUCTION

Osteoporosis is a highly prevalent disease with significant socioeconomic burden, and its incidence will further increase due to a longer life expectancy and an aging population (Burge et al., 2007; Hernlund et al., 2013; US Department of Health and Human Services, 2004). Postmenopausal osteoporosis, which results from the decline in estrogen levels after menopause, is the most common form of osteoporosis (van Staa et al., 2001). The rapid and progressive loss of bone after menopause occurs as a result of an imbalanced bone turnover with bone resorption exceeding bone formation. Thus, anti-resorptive drugs are most commonly used to prevent bone loss and reduce fracture risk in affected patients (Rachner et al., 2011). However, besides directly affecting bone cells, estrogen deficiency also impacts lymphocyte differentiation and function, which may also contribute to pathogenesis of osteoporosis by negatively affecting the communication with osteoblasts and osteoclasts. In fact, estrogen deficiency leads to an expansion of B and T cell populations in mice (Cenci et al., 2003; Fujiwara et al., 2016; Garcia-Perez et al., 2005; Qiu et al., 2016). However, the role of B and T cells in estrogen-deficiency-induced bone loss remains controversial (Masuzawa et al., 1994; Miyaura et al., 1997). Although one study showed that B cells contribute to estrogen-deficiency-induced bone loss via their production of receptor activator of NF-κB ligand (RANKL) (Onal et al., 2012), another study completely depleted mature B cells and showed that these mice lost equal amounts of bone as their B cell replete controls (Li et al., 2007a). Similarly, although some studies show that both T-cell-deficient nude mice and T-cell-depleted wild-type mice fail to respond to ovariectomy with bone loss (8–12), another study using three different T-cell-deficient mouse models showed similar bone loss after ovariectomy as their corresponding controls (Lee et al., 2006). Of those studies that showed a critical role of lymphocytes in estrogen-deficiency-induced bone loss, the increased production of osteoclast stimulating factors such as RANKL, TNF-α, IL-6, and IL-17 by lymphocytes was proposed as a mechanism (Cenci et al., 2000, 2003; Roggia et al., 2001; Takayanagi, 2007). Mechanisms of T-cell-produced factors on osteoblasts, however, remain largely undefined, especially in the context of estrogen deficiency.

Previous evidence indicates that T cells can produce Wnt10b to amplify the osteo-anabolic effects of parathyroid hormone treatment (Bedi et al., 2012; Terauchi et al., 2009). T cells were recently also shown to express Dickkopf-1 (DKK1) (Chae et al., 2017), a potent Wnt inhibitor, which binds to the Wnt co-receptors LDL receptor–related protein 5 and 6 (LRP5/6) and thereby blocks further interactions with Wnt ligands

[1]Department of Medicine III, Division of Endocrinology, Diabetes and Bone Diseases, Technische Universität Dresden, Dresden 01307, Germany

[2]Center for Healthy Aging, Technische Universität Dresden, Dresden, Germany

[3]Center for Regenerative Therapies Dresden, Technische Universität Dresden, Dresden, Germany

[4]Division of Molecular Embryology, DKFZ-ZMBH Alliance, Heidelberg, Germany

[5]Institute of Molecular Biology, Mainz, Germany

[6]Lead contact

*Correspondence: martina.rauner@ukdd.de

https://doi.org/10.1016/j.isci.2021.102224

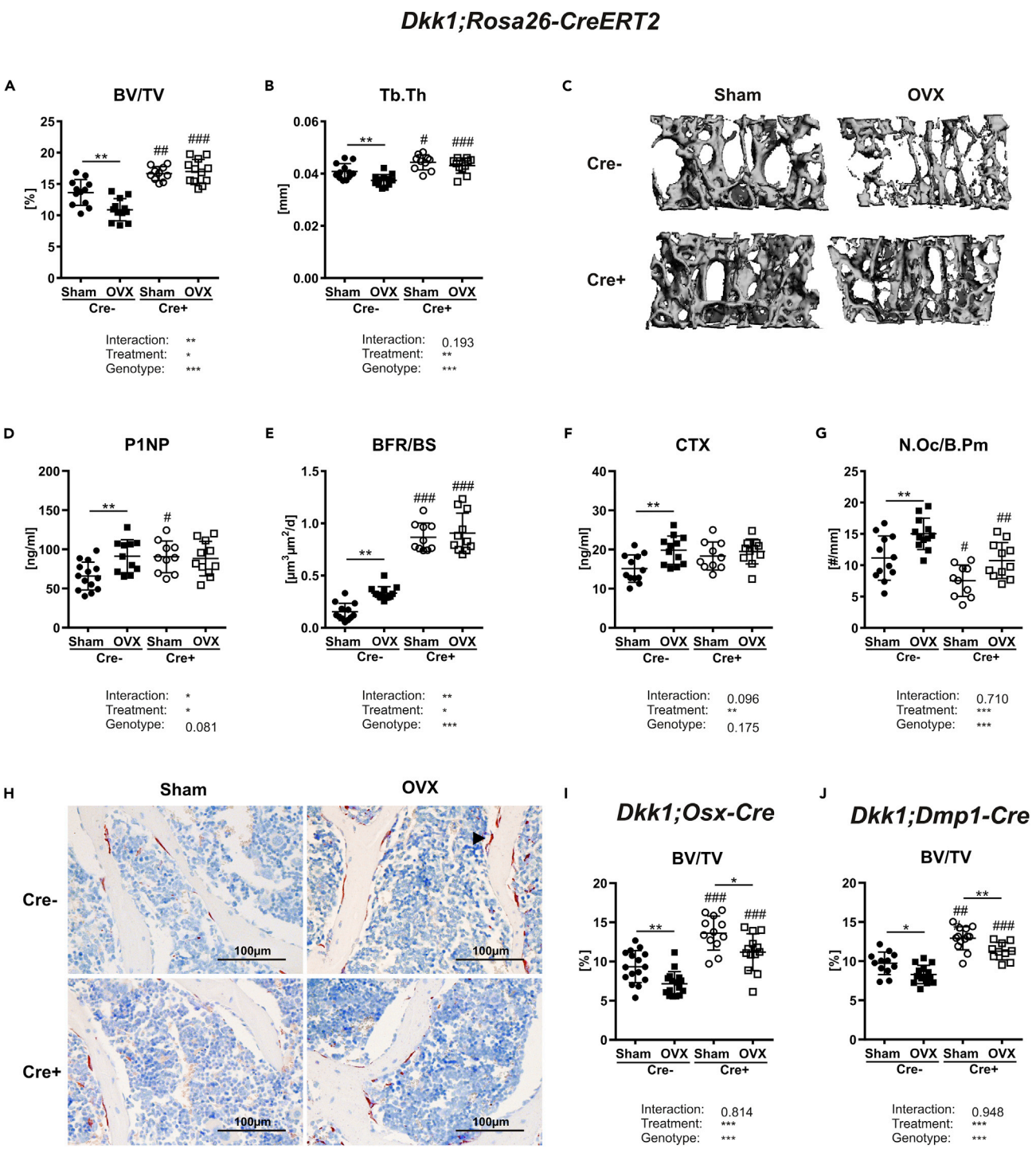

Figure 1. Global, but not osteogenic, *Dkk1* deletion protects against estrogen-deficiency-induced bone loss

The fourth vertebral body of 14-week-old female Sham operated or ovariectomized (OVX) *Dkk1*$^{fl/fl}$;*Rosa26-ERT2-Cre* and respective Cre-negative control mice were analyzed by µCT.

(A and B) (A) Trabecular bone volume per total volume (BV/TV) and (B) trabecular thickness (Tb.Th) of fourth vertebral body.

(C) Representative 3D reconstruction of the analyzed fourth vertebral body.

(D and E) (D) Serum levels of the Wnt inhibitors dickkopf-1 (DKK1) and (E) bone formation marker procollagen type 1 amino-terminal propeptide (P1NP) were analyzed using commercially available ELISA.

(F) Histomorphometric analysis of calcein double staining was performed to determine the (F) bone formation rate/bone surface (BFR/BS).

Figure 1. *Continued*

(G) Serum level of bone resorption marker (G) carboxy-terminal collagen crosslinks (CTX) was measured using a commercially available ELISA.

(H) The fourth vertebral body was stained with tartrate-resistant acid phosphatase (TRAP) to determine the osteoclast number per bone parameter (N.Oc/B.Pm). Cre− Sham, n = 12; Cre− OVX, n = 12; Cre+ Sham, n = 10; Cre+ OVX, n = 12.

(I) Representative images (20x) of histological sections of fourth vertebral body stained with TRAP (arrow indicates osteoclast). The fourth vertebral body of 14-week-old female Sham operated or ovariectomized *Dkk1*$^{fl/fl}$;*Osx-Cre* (Cre− Sham, n = 16; Cre− OVX, n = 16; Cre+ Sham, n = 12; Cre+ OVX, n = 13) and *Dkk1*$^{fl/fl}$;*Dmp1-Cre* mice (Cre− Sham, n = 13; Cre− OVX, n = 15; Cre+ Sham, n = 13; Cre+ OVX, n = 10), and respective controls were analyzed to assess (J-M) trabecular bone volume per total volume (BV/TV) and serum levels of DKK1. Data represent the mean ± SD. Statistical analysis was performed by the two-way ANOVA. *p < 0.05, **p < 0.01, ***p < 0.001 versus Sham or #p < 0.05, ##p < 0.01, ###p < 0.001 versus respective Cre-negative control.

(Bhat et al., 2007; Mao et al., 2001, 2002). By blocking Wnt signaling, DKK1 negatively regulates osteoblast differentiation and function, and it stimulates osteoclastogenesis indirectly via the increased production of RANKL and lower production of osteoprotegerin (OPG) in osteoblasts. Thus, DKK1 is a potent negative regulator of bone mass (Li et al., 2006; Morvan et al., 2006). DKK1 is expressed in various organs (bone, brain, reproductive system, kidney/urogenital tract) and by several cell types within bone (Christodoulides et al., 2006; Li et al., 2006; Pietilä et al., 2011), whereas osterix-expressing osteoprogenitors appear to be the main source of circulating DKK1 levels (Colditz et al., 2018). Interestingly, increased DKK1 expression is observed in various bone-related disorders, including rheumatoid arthritis (Diarra et al., 2007), glucocorticoid-induced osteoporosis (Rauner et al., 2013; Wang et al., 2008), and malignant bone disease (Rachner et al., 2014; Tian et al., 2003). Blocking DKK1 using monoclonal antibodies or genetic approaches protects mice from arthritis- (Diarra et al., 2007), GC-, and myeloma-induced bone loss (Colditz et al., 2019; Pozzi et al., 2013). Even though DKK1 levels are also increased in osteoporotic postmenopausal women (Ahmed et al., 2013), it has remained unclear whether DKK1 mediates bone loss due to estrogen deficiency and if so, whether its expression in T cells also contributes to this effect.

In this study, we generated global, osteoblast, osteocyte, and T-cell-specific *Dkk1* knock-out mice to determine if and how DKK1 contributes to estrogen-deficiency-induced bone loss. Although global and T-cell-specific *Dkk1* deletion protected mice from estrogen-deficiency-induced bone loss, lack of *Dkk1* in the osteogenic lineage did not. Indirect co-culture experiments revealed that activated T cells suppressed osteoblast differentiation via inhibiting Wnt signaling. Importantly, lack of Dkk1 expression in T cells did not only mediate pathological bone loss but also controlled physiological bone remodeling. Thus, our findings underline the critical role of T cells in skeletal health and disease.

RESULTS

Global loss of *Dkk1* protects against estrogen-deficiency-induced bone loss

In order to assess the contribution of DKK1 in the pathogenesis of estrogen-deficiency-induced bone loss, we deleted *Dkk1* in *Dkk1*$^{fl/fl}$;*Rosa26-CreERT2* mice with tamoxifen and induced bone loss by OVX. The success of the procedure was confirmed by weighing the uterine, which was significantly atrophied in the OVX groups (data not shown).

Dkk1-proficient Cre− mice showed a significant reduction of vertebral trabecular bone volume (−20%) and trabecular thickness (−8%) four weeks after OVX, whereas global *Dkk1* conditional knock-out (cKO) mice were protected from OVX-induced bone loss (Figures 1A and 1B). Trabecular number and trabecular separation were not significantly altered in both genotypes (Table 1). Representative 3D reconstructions of the fourth vertebrae body are shown in Figure 1C. As DKK1 was recently shown to be upregulated in bone after OVX in rats and in serum from women suffering from postmenopausal osteoporosis (Ahmed et al., 2013; Tian et al., 2015), we analyzed skeletal *Dkk1* mRNA levels in our mice. *Dkk1* mRNA levels were higher in bone tissue from ovariectomized control mice, whereas *Dkk1* was not detected in the bone tissue of cKO mice (Figure S1). The deletion of *Dkk1* led to higher skeletal expression of the Wnt target genes *Lef1* and *Axin2*, and both were decreased after OVX in both genotypes (Figure S1).

As a significant proportion of women with postmenopausal osteoporosis show enhanced bone turnover (Eastell et al., 2016), we determined bone turnover after OVX. As expected, OVX increased both bone formation and bone resorption parameters in Cre− wild-type mice. OVX increased P1NP serum levels (+39%), the mineral apposition rate (+28%), and the bone formation rate (+116%) in control mice, whereas these parameters were not altered in global *Dkk1* cKO mice (Figures 1D and 1E, Table 1). Interestingly, estrogen withdrawal only enhanced osteoblast activity but not osteoblast and osteocyte numbers (Table 1). In

Table 1. Bone phenotype of third and fourth vertebral body from 14-week-old female sham versus ovariectomized (OVX) *Dkk1*$^{fl/fl}$;*Rosa26-CreERT2*, *Dkk1*$^{fl/fl}$;*Osx-Cre* and *Dkk1*$^{fl/fl}$;*Dmp1-Cre* mice

Spine	Cre− Sham	OVX	p value and % change	Cre+ Sham	OVX	p value and % change
Dkk1*$^{fl/fl}$;*Rosa26-CreERT2	**n = 12**	**n = 12**		**n = 10**	**n = 12**	
μCT						
Tb.N [1/mm]	3.87 ± 0.35	3.61 ± 0.19	0.225–7%	4.38 ± 0.32$^{\#\#}$	4.17 ± 0.34$^{\#\#\#}$	0.682–5%
Tb.Sp [mm]	0.25 ± 0.03	0.27 ± 0.02	0.647 + 8%	0.24 ± 0.04	0.26 ± 0.02	0.567 + 8%
Histomorphometry						
MS/BS [%]	17.7 ± 4.02	20.0 ± 2.75	0.787 + 13%	18.6 ± 1.91	20.1 ± 4.51	>0.999 + 8%
MAR [μm/day]	1.26 ± 0.15	1.61 ± 0.25	<0.05 + 28%	1.69 ± 0.25$^{\#\#}$	1.92 ± 0.34	0.351 + 13%
N.Ob/B.Pm [#/mm]	11.9 ± 3.45	12.4 ± 3.39	>0.999 + 4%	13.1 ± 2.80	14.2 ± 4.05	>0.999 + 8%
N.Ot/B.Ar [#/mm^2]	152 ± 49.2	184 ± 28.8	0.228 + 17%	252 ± 34.4$^{\#\#\#}$	244 ± 19.8$^{\#\#}$	>0.999–3%
Dkk1*$^{fl/fl}$;*Osx-Cre	**n = 16**	**n = 16**		**n = 12**	**n = 13**	
μCT						
Tb.Th [mm]	40.4 ± 2.28	36.7 ± 2.42	<0.01–9%	41.4 ± 3.01	38.2 ± 2.31	<0.05–8%
Tb.N [1/mm]	3.56 ± 0.41	3.22 ± 0.27	<0.05–10%	4.02 ± 0.24$^{\#\#}$	3.67 ± 0.23$^{\#\#}$	<0.05–9%
Tb.Sp [mm]	0.28 ± 0.03	0.31 ± 0.02	<0.05 + 11%	0.25 ± 0.02$^{\#\#}$	0.27 ± 0.02$^{\#\#}$	<0.05 + 8%
Histomorphometry						
MS/BS [%]	25.2 ± 5.31	29.1 ± 4.60	0.246 + 15%	28.2 ± 4.21	28.6 ± 3.72	+1%
MAR [μm/day]	1.49 ± 0.45	2.29 ± 0.55	<0.05 + 54%	2.44 ± 0.91$^{\#\#}$	3.30 ± 0.90$^{\#\#}$	<0.05 + 35%
BFR/BS [μm^3/μm^2/day]	0.40 ± 0.16	0.75 ± 0.33	<0.05 + 88%	0.78 ± 0.38$^{\#}$	1.15 ± 0.30$^{\#\#}$	<0.05 + 47%
N.Ob/B.Pm [#/mm]	16.2 ± 3.03	17.2 ± 2.56	>0.999 + 6%	16.4 ± 2.72	16.5 ± 3.54	>0.999 + 1%
N.Oc/B.Pm [#/mm]	7.06 ± 1.84	8.91 ± 1.77	<0.05 + 26%	4.39 ± 1.09$^{\#\#\#}$	6.24 ± 1.67$^{\#\#\#}$	<0.05 + 42%
Dkk1*$^{fl/fl}$;*Dmp1-Cre	**n = 13**	**n = 15**		**n = 13**	**n = 10**	
μCT						
Tb.Th [mm]	41.0 ± 3.64	38.4 ± 2.85	0.087–6%	42.7 ± 2.24	39.6 ± 1.70	0.066–7%
Tb.N [1/mm]	3.70 ± 0.33	3.29 ± 0.32	<0.05–11%	4.10 ± 0.32$^{\#}$	3.71 ± 0.33$^{\#}$	<0.05–10%
Tb.Sp [mm]	0.28 ± 0.02	0.31 ± 0.03	<0.01 + 11%	0.25 ± 0.02$^{\#}$	0.28 ± 0.03$^{\#}$	<0.05 + 12%
Histomorphometry						
MS/BS [%]	28.9 ± 3.60	30.1 ± 2.60	>0.999 + 4%	28.9 ± 3.57	29.9 ± 2.62	>0.999 + 3%
MAR [μm/day]	1.39 ± 0.23	1.95 ± 0.44	<0.01 + 40%	1.96 ± 0.36$^{\#\#}$	2.42 ± 0.34$^{\#}$	<0.05 + 23%
BFR/BS [μm^3/μm^2/day]	0.37 ± 0.17	0.62 ± 0.16	<0.05 + 68%	0.70 ± 0.24$^{\#\#}$	1.03 ± 0.22$^{\#\#\#}$	<0.01 + 47%
N.Ob/B.Pm [#/mm]	23.2 ± 3.36	23.7 ± 3.06	>0.999 + 2%	23.6 ± 4.51	24.6 ± 3.58	>0.999 + 4%
N.Oc/B.Pm [#/mm]	8.02 ± 2.00	11.2 ± 2.58	<0.001 + 40%	5.90 ± 1.28$^{\#}$	8.47 ± 1.30$^{\#\#}$	<0.05 + 44%

Tb.Th = trabecular thickness, Tb.N = trabecular number, Tb.Sp = trabecular separation, MS/BS = mineralizing surface/bone surface, MAR = mineral apposition rate, BFR/BS = bone formation rate/bone surface, N.Ob/B.Pm = number of osteoblasts, N.Oc/B.Pm = number of osteoclasts/bone perimeter, N.Ot/B.Ar = number of osteocytes/bone area. Data represent the mean ± SD. Statistical analysis was performed using the two-way ANOVA. $^{\#}p < 0.05$, $^{\#\#}p < 0.01$, $^{\#\#\#}p < 0.001$ versus respective Cre-negative control.

addition, the bone resorption marker CTX, the number of osteoclasts, and *Rankl* expression in bone was increased only in ovariectomized control mice but were not significantly changed in cKO mice (Figures 1F, 1G, and S1). *Opg* expression was highly increased in the bones of cKO mice but did not change after OVX in either genotype (Figure S1). Representative images of TRAP-stained bone sections are depicted in Figure 1H. Taken together, *Dkk1* plays a critical role in OVX-induced bone loss.

Lack of *Dkk1* in osteolineage cells has no influence on estrogen-deficiency-induced bone loss

To determine whether osteoprogenitors or osteocytes contribute to OVX-induced bone loss via their production of DKK1, *Dkk1*$^{fl/fl}$;*Osx-Cre* and *Dkk1*$^{fl/fl}$;*Dmp1-Cre* mice were subjected to OVX. In contrast to

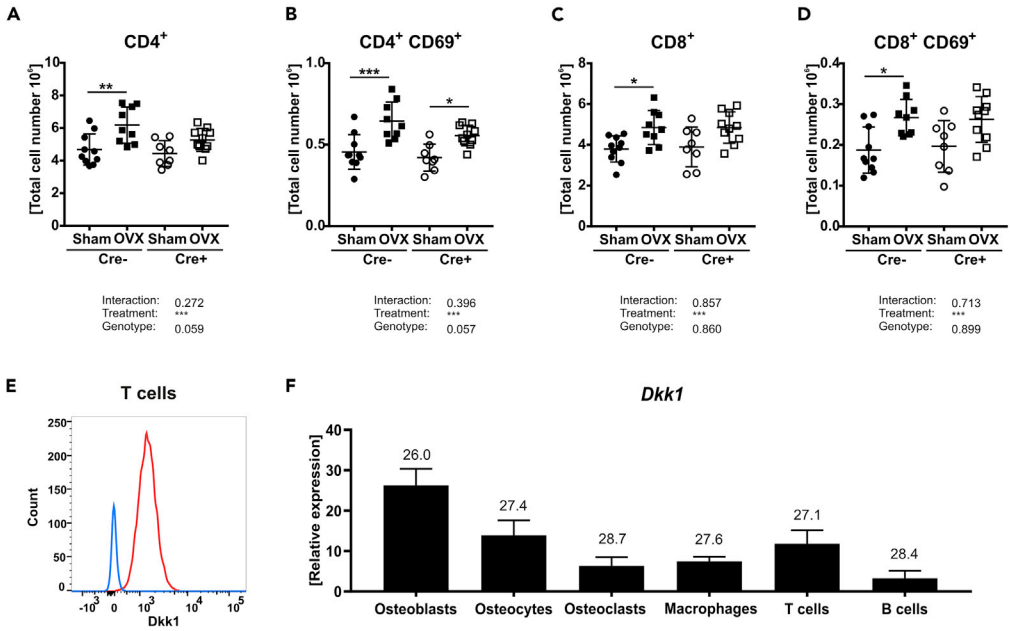

Figure 2. Estrogen-deficiency is associated with an increased number of activated T cells

Absolute numbers of splenic T lymphocyte populations of Sham versus OVX-operated 14-week-old *Dkk1*$^{fl/fl}$;*Rosa26-CreERT2* and control mice were determined using FACS analysis.

(A–D) (A) T helper cells, (B) activated T helper cells, (C) cytotoxic T cells, and (D) activated cytotoxic T cells were determined by their specific indicated surface markers. Cre− Sham, n = 10; Cre− OVX, n = 9; Cre+ Sham, n = 8; Cre+ OVX, n = 10.

(E) Intracellular DKK1 staining of wild-type-derived splenic T cells was measured using FACS analysis. n = 4 animals per group.

(F) Real-time PCR analysis was performed for *Dkk1* mRNA expression in different cell types. n = 5 animals per group. Gene expression levels were normalized to *β-Actin*. Data represent the mean ± SD. Numbers in graph indicate threshold values at constant *β-Actin*. Statistical analysis was performed by the two-way ANOVA. *p < 0.05, **p < 0.01, ***p < 0.001 versus Sham (Cre− or Cre+) and #p < 0.05, ##p < 0.01, ###p < 0.001 versus Cre-negative control.

Dkk1$^{fl/fl}$*;Rosa26-CreERT2 mice, Dkk1*$^{fl/fl}$*;Osx-Cre and Dkk1*$^{fl/fl}$*;Dmp1-Cre* mice lost similar amounts of bone after OVX as their controls (Figures 1I and 1J). Moreover, all genotypes showed similar alterations in bone microarchitecture (Table 1). Finally, histomorphometric analysis confirmed that *Dkk1*$^{fl/fl}$*;Osx-Cre and Dkk1*$^{fl/fl}$*;Dmp1-Cre* mice showed similar alterations in bone turnover after OVX as their wild-type littermate controls (Table 1).

Estrogen deficiency is associated with increased proliferation and activation of T cells

As estrogen deficiency is associated with an increased number of T cells and T cells have been reported to alter bone metabolism via their production of Wnt10b (Pacifici, 2012), we investigated whether T cells also use DKK1 to modulate bone turnover in estrogen deficiency. First, we assessed whether OVX also activates T cells in our model. Flow cytometric analyses revealed an increased number of total splenic T cells in all three mouse lines (*ERT2-Cre, Osx-Cre, Dmp1-Cre*) after OVX (Table S1). However, this increase was less pronounced in global cKO (Table S1). When we analyzed T lymphocyte subsets, global cKO mice failed to significantly increase CD4$^+$ (T helper cells) and CD8$^+$ (cytotoxic T lymphocyte) T cell numbers after OVX, whereas mice that lacked *Dkk1* in osteogenic cells showed similar increase as their Cre− controls (Table S1). Furthermore, OVX led to an activation of CD4$^+$ and to a lesser extent of CD8$^+$ T cells in Cre-negative controls, which was apparent by the increase of the CD69$^+$ cell fraction (Figures 2A–2D and Table S1) (Ziegler et al., 1994). Similar increases were found in *Dkk1*$^{fl/fl}$*;Osx-Cre* and *Dkk1*$^{fl/fl}$*;Dmp1-Cre* mice (Table S1). Surprisingly, global deletion of *Dkk1* mitigated the OVX-induced activation of CD4$^+$ and CD8$^+$ T cells (Figures 2B and 2D). Apart from T cells, we also investigated the total number of B cells (CD45R$^+$) in the spleen and myeloid-derived suppressor cells (CD11b$^+$GR1$^+$) in the bone marrow. However, total numbers of both cell populations were unaltered after OVX (Table S1).

Finally, we examined whether T cells express DKK1. Flow cytometric analysis revealed that wild-type T cells exhibit DKK1 expression (Figure 2E). In addition, qPCR analysis confirmed that T cells express *Dkk1*, albeit to a lesser degree than osteoblasts (Figure 2F).

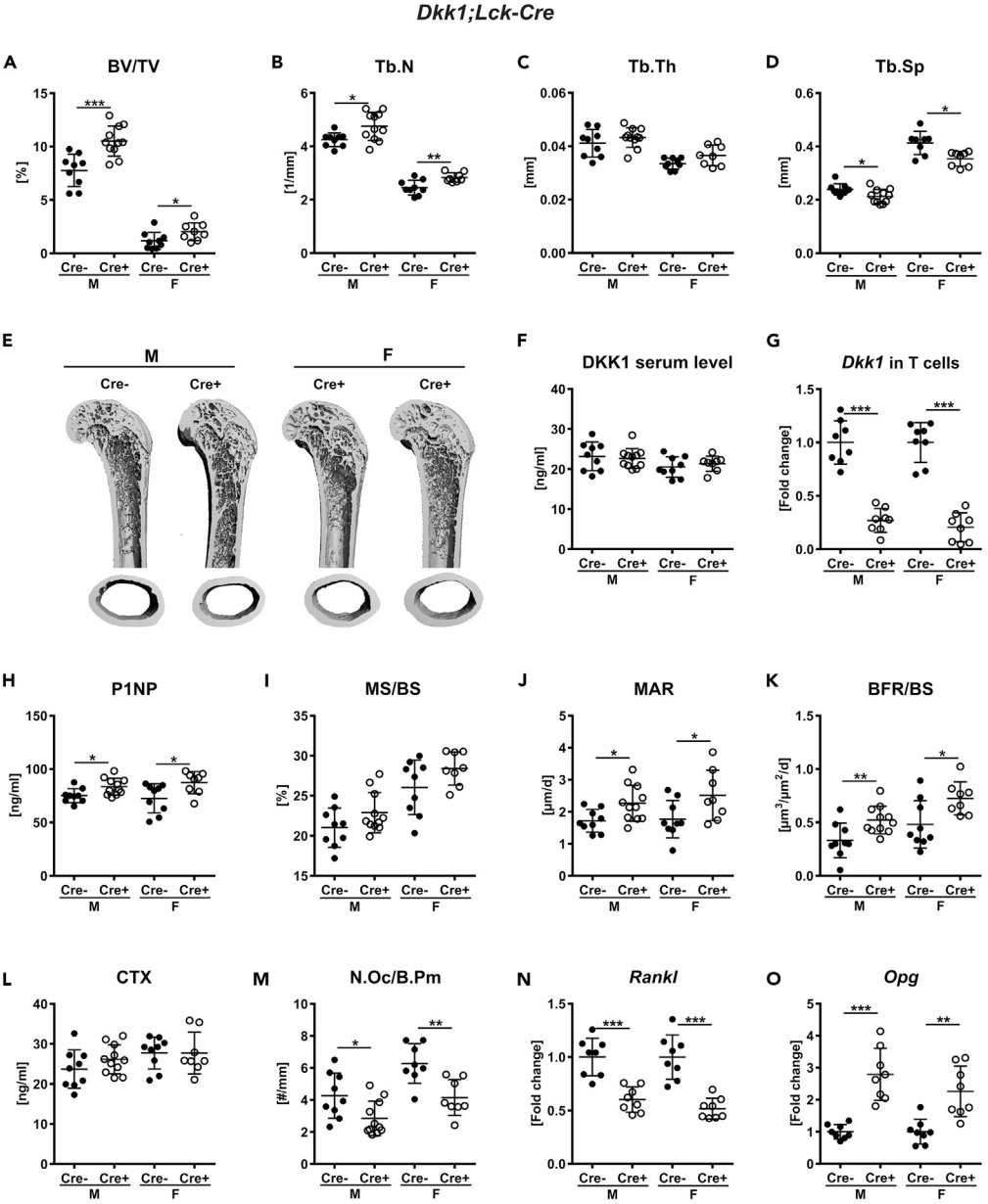

Figure 3. Lack of *Dkk1* in T cells (*Lck-Cre*) increases bone volume

The fourth vertebral body of 12-week-old male and female *Dkk1*$^{fl/fl}$;*Lck-Cre* (Cre-positive and Cre-negative) mice were analyzed by µCT.

(A–D) (A) Trabecular bone volume per total volume (BV/TV), (B) trabecular number (Tb.N), (C) trabecular thickness (Tb.Th), and (D) trabecular separation (Tb.Sp) of the fourth vertebral body.

(E) Representative 3D reconstruction of the analyzed fourth vertebral body. Cre− male, n = 9; Cre+ male, n = 11; Cre−female, n = 9; Cre+ female, n = 8.

(F and G) (F) DKK1 Serum levels (Cre− male, n = 9; Cre+ male, n = 11; Cre− female, n = 9; Cre+ female, n = 8) were assessed using a commercially available ELISA, and (G) real-time PCR analysis was performed for *Dkk1* mRNA expression in T cells (n = 8 animals per group). Histomorphometric and serum osteoblast and osteoclast parameters of 12-week-old male and female *Dkk1*$^{fl/fl}$;*Lck-Cre mice* and littermate controls were analyzed.

(H–K) (H) Quantification of serum procollagen type 1 amino-terminal propeptide (P1NP) was performed by ELISA. Histomorphometric analysis of calcein double staining was performed to determine the (I) mineralizing surface/bone surface (MS/BS), (J) mineral apposition rate (MAR), and (K) bone formation rate/bone surface (BFR/BS).

(L) Serum carboxy-terminal collagen crosslinks (CTX) were measured using ELISA.

Figure 3. *Continued*

(M) Tartrate-resistant acid phosphatase (TRAP) staining was used to determine the number of osteoclast/bone parameter (N.Oc/B.Pm). Cre− male, n = 9; Cre+ male, n = 11; Cre− female, n = 9; Cre+ female, n = 8.

(N and O) (N) Receptor activator of nuclear factor-κB ligand (*Rankl*) and (O) osteoprotegerin (*Opg*) mRNA expression in femoral bone tissue were analyzed using real-time PCR analysis. n = 8 animals per group. Gene expression levels were normalized to *β-Actin*. Data represent the mean ± SD. Statistical analysis was performed by the Student's t test. *p < 0.05, **p < 0.01, ***p < 0.001 versus Cre-negative control.

T-cell-specific *Dkk1* deletion increases bone mass

As T cells express DKK1, we next investigated whether T-cell-derived DKK1 can influence bone remodeling. To test this, we generated *Dkk1*$^{fl/fl}$*;Lck-Cre* mice, which express *Cre* under the control of the *Lck* (lymphocyte protein tyrosine kinase) promoter, enabling T-cell-specific excision of *Dkk1* (Baumann et al., 2005). Recombination of the floxed *Dkk1* allele was only found in MACS-purified T cells from *Dkk1*$^{fl/fl}$*;Lck-Cre* mice but not in any other organ investigated (Figure S2A). *Dkk1*$^{fl/fl}$*;Lck-Cre* and Cre− control mice were born at a Mendelian ratio with no abnormalities in size and body weight (Figure S2B). Twelve-week-old male and female *Dkk1*$^{fl/fl}$*;Lck-Cre* mice showed an increased bone volume at the fourth lumbar vertebrae and distal femur (Figure 3A and Table S2). At the structural level, the fourth vertebral body had a higher trabecular number (male: +11%, female: +10%), whereas trabecular thickness was unchanged and trabecular separation was significantly lower (male: −10%, female: −11%) (Figures 3B–3D). T-cell-specific *Dkk1* deletion had no effect on the cortical compartment (BMD: male: Cre−: 923 ± 40.4, Cre+: 918 ± 37.8; female: Cre−: 923 ± 37.5, Cre+: 923 ± 44.3). The distal femur showed a similar pattern, and the data are summarized in Table S2. Representative 3D reconstructions of the femur are depicted in Figure 3E. Interestingly, DKK1 serum levels (Figure 3F) as well as mRNA expression in the femora of *Dkk1*$^{fl/fl}$*;Lck-Cre* mice were not altered (bone: male: Cre−: 1.00 ± 0.09, Cre+: 0.97 ± 0.04; female: Cre−: 1.00 ± 0.05, Cre+: 1.07 ± 0.04). However, *Dkk1* mRNA expression was reduced by 73%–79% in MACS-purified T cells (Figure 3G).

We next determined whether the high bone mass in *Dkk1*$^{fl/fl}$*;Lck-Cre* is also due to increased bone formation as previously shown in cKO mice lacking *Dkk1* globally or in osteogenic cells (Colditz et al., 2018). Lack of *Dkk1* in T cells resulted in higher P1NP serum levels (male: +11%, female: +22%), an increased mineral apposition rate, and a higher bone formation rate at the vertebra in both sexes (Figures 3H–3K). Mineralizing surface was not altered in *Dkk1*$^{fl/fl}$*;Lck-Cre* mice (Figure 3I). The femora of Cre-positive mice showed a similar increase in bone formation parameters (Table S2). Similar to mice lacking *Dkk1* globally or in cells of the osteogenic lineage, T-cell-specific *Dkk1* deletion had no effect on serum CTX levels, whereas the number of osteoclasts was significantly reduced in the axial and appendicular skeleton (Figures 3L-M, Table S2). However, the reduced number of osteoclasts was associated with a decrease in TRAP5b serum levels (male: Cre−: 9.92 ± 0.21, Cre+: 8.60 ± 0.44; female: Cre−: 9.70 ± 0.32, Cre+: 8.50 ± 0.44). In line with this, *Rankl* expression was decreased, whereas *Opg* expression was increased in the bones of *Dkk1*$^{fl/fl}$*;Lck-Cre* mice (Figures 3N-O).

Because T-cell-derived DKK1 has been shown to modify T cell activation (Chae et al., 2017), which may impact on bone remodeling as well, and the *Lck-cre* has been shown to alter the T cell phenotype (Carow et al., 2016), we investigated the T cell phenotype in *Dkk1*$^{fl/fl}$*;Lck-Cre* mice and *Dkk1*$^{fl/fl}$*;Rosa26-CreERT2* mice in more detail using FACS analysis (Table S3). Global or T-cell-specific *Dkk1* deletion did not alter the cellularity of the thymus and spleen. Furthermore, CD69 expression and the number of major T cell subsets, including Treg cells, which have been shown to express high DKK1 levels (Chae et al., 2017), did not differ in *Dkk1*$^{fl/fl}$*;Lck-Cre* mice. In case of *Dkk1*$^{fl/fl}$*;Rosa26-CreERT2* mice only the number of double-negative $CD4^{-}CD8^{-}$ cells was significantly reduced. Hence alterations in the T cell phenotype are not the cause of the bone phenotype seen in *Dkk1*$^{fl/fl}$*;Lck-Cre* mice.

Taken together, our data show that T-cell-specific deficiency of *Dkk1* contributes to the maintenance of bone remodeling by controlling bone formation and osteoclast numbers in both sexes.

Transfer of wild-type T cells rescues the high bone mass of T-cell-specific *Dkk1* cKO mice

We next investigated whether the changes in bone remodeling in *Dkk1*$^{fl/fl}$*;Lck-Cre* mice can be rescued by transplanting *Dkk1*-proficient wild-type T cells (Ly5.1 mice) into those mice. Therefore, MACS-purified T cells were transplanted into 9-week-old female *Dkk1*$^{fl/fl}$*;Lck-Cre* mice and their littermate controls. All mice tolerated this procedure and showed no signs of immune response. After 3 weeks, bone parameters

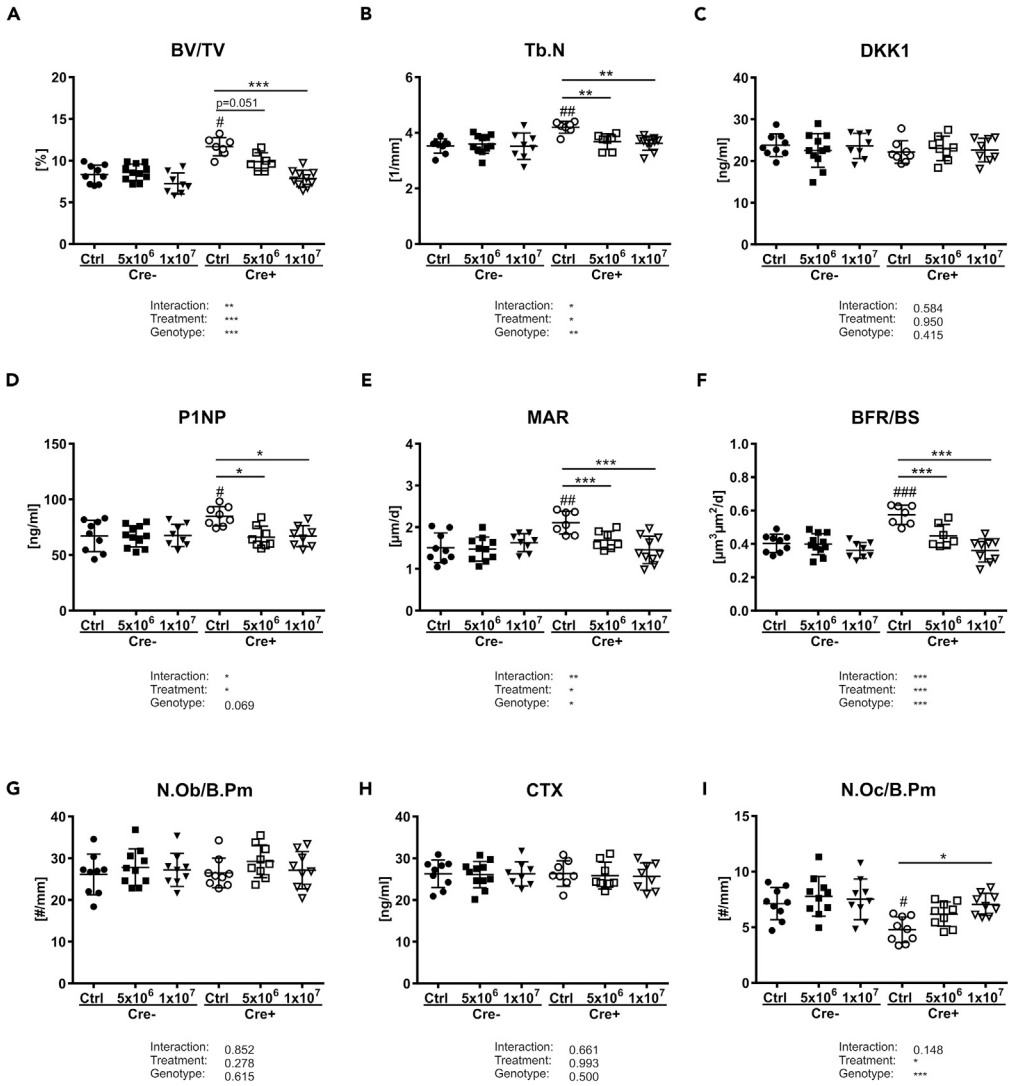

Figure 4. Transplantation of T cells abolishes the positive effect of T-cell-specific *Dkk1* deletion on bone

The fourth vertebral bodies of 13-week-old female *Dkk1*$^{fl/fl}$*;Lck-Cre* (Cre-positive and Cre-negative) mice were analyzed 3 weeks after transplantation of wild-type-derived T cells by µCT.

(A and B) (A) Trabecular bone volume per total volume (BV/TV) and (B) trabecular number (Tb.N) of the fourth vertebral body.

(C–F) Quantification of serum (C) DKK1 and (D) procollagen type 1 amino-terminal propeptide (P1NP) was performed by ELISA. Cre− Ctrl, n = 9; Cre− 5x10^6, n = 11; Cre− 1x10^7, n = 8; Cre+ Ctrl, n = 8; Cre+ 5x10^6, n = 8; Cre+ 1x10^7, n = 9. Histomorphometric analysis of calcein double staining was performed to determine bone mineralizing surface/bone surface (MS/BS) and (F) formation rate/bone surface (BFR/BS). Cre− Ctrl, n = 9; Cre− 5x10^6, n = 10; Cre− 1x10^7, n = 8; Cre+ Ctrl, n = 7; Cre+ 5x10^6, n = 7; Cre+ 1x10^7, n = 9.

(G) Tartrate-resistant acid phosphatase (TRAP) staining was used to determine the number of osteoblast/bone parameter (N.Ob/B.Pm).

(H and I) (H) Serum carboxy-terminal collagen crosslinks (CTX) were measured using ELISA, and (I) the number of osteoclast/bone parameter (N.Oc/B.Pm) was assessed using TRAP staining. Cre− Ctrl, n = 9; Cre− 5x10^6, n = 11; Cre− 1x10^7, n = 8; Cre+ Ctrl, n = 8; Cre+ 5x10^6, n = 8; Cre+ 1x10^7, n = 9. Data represent the mean ± SD. Statistical analysis was performed by the two-way ANOVA. *p < 0.05, **p < 0.01, ***p < 0.001 versus untransplanted control (Cre− or Cre+) and #p < 0.05, ##p < 0.01, ###p < 0.001 versus untransplanted Cre− control.

were assessed. In Cre− control mice, transplantation did not influence any of the investigated bone parameters, whereas *Dkk1*$^{fl/fl}$*;Lck-Cre* mice, which were injected with 5 × 10^6 T cells, showed slightly reduced bone volume and trabecular number (Figures 4A and 4B). This effect on bone was even more pronounced

when mice were injected with a higher number of T cells, resulting in a significant reduction of bone volume and trabecular number (Figures 4A and 4B). No alterations in DKK1 serum levels were detected after transplantation (Figure 4C). The reduced bone mass in transplanted *Dkk1*$^{fl/fl}$;*Lck-Cre* mice was triggered by reduced bone formation, which is evident by reduced P1NP serum levels and decreased mineral apposition and bone formation rates, whereas number of osteoblasts was not altered (Figures 4D–4G). Even though T cell transfer did not affect CTX serum levels, it increased the number of osteoclasts in *Dkk1*$^{fl/fl}$;*Lck-Cre* reaching similar numbers as their Cre− controls (Figures 4H and 4I). Comparable results were found when T cells were transplanted into male mice (date not shown). Thus, these results indicate an important role of alterations that occur as a result of T-cell-deficiency of DKK1 for physiologic bone remodeling.

T cells affect osteoblast differentiation depending on their activation status

To explore how secreted proteins from T cells influence osteoblast function, conditioned medium (CM) was collected from T cells that were isolated from the spleen of wild-type mice and treated with anti-CD3 (active T cells) or without anti-CD3 (inactive T cells) for 72 h. Afterward CM was used for indirect co-culture experiments with primary osteoblasts. After 7 days of differentiation with different ratios of CM, osteoblasts exposed to CM from inactive T cells had a 2-fold higher expression of *Osx*, *Alp*, and *Ocn*, whereas *Runx2* was not altered (Figures 5A–5D). In contrast, CM from activated T cells inhibited gene expression of *Runx2*, *Osx*, *Alp*, and *Ocn* in a dose-dependent manner, with 75% CM showing the highest inhibition. This suggests that depending on the activation status, T-cell-derived CM can influence osteogenic differentiation.

As estrogen deficiency is associated with an increased T cell activation, we determined whether the activation status of T cells influences *Dkk1* gene expression in osteoblasts. CM from activated T cells increased *Dkk1* expression in osteoblasts in a dose-dependent manner (Figure 5E). At the same time, expression levels of the Wnt target genes *Opg*, *Lef1*, and *Axin2* were reduced (Figures 5F–5H). In line with that finding, CM from activated T cells also suppressed Wnt3a-induced TCF/LEF Wnt promoter activity (Figure S3). CM from inactive T cells led to an upregulation of Wnt target genes in osteoblasts and Wnt promoter activity (Figures 5F–5H, and Figure S3). Interestingly, activation of T cells also increased their own *Dkk1* mRNA expression by 2-fold (inactive: 1.00 $\pm$ 0.02, active: 2.05 $\pm$ 0.42). These results indicate that T cells differentially influence osteoblast differentiation depending on their activation status.

Lack of *Dkk1* in T cells diminishes their effect on osteoblast differentiation

To determine whether DKK1 mediates the negative effects of activated T cells on osteoblasts, we collected CM from T cells isolated from *Dkk1*$^{fl/fl}$;*Rosa26-ERT2-Cre* and control mice 3 weeks after tamoxifen injections. Successful deletion of *Dkk1* in T cells was confirmed by qPCR of purified T cells (Figure S4). Similar to wild-type-derived CM, osteoblasts that were treated with CM derived from inactive *Dkk1*-expressing T cells (Cre−) showed an increased expression of osteogenic genes (*Osx*, *Alp*, and *Ocn*), whereas CM from activated T cells had the opposite effect (Figures 5I–5L). However, when *Dkk1* was deleted in T cells (Cre+) the positive effect of CM from inactive T cells persisted, whereas the negative effect of activated T cells on osteoblast differentiation was fully abolished (Figures 5I–5L). The same was true for *Dkk1*, which was only increased in osteoblasts that were treated with CM derived from activated *Dkk1*-expressing T cells (Figure 5M). Inhibited Wnt signaling, reflected by reduced expression of *Opg*, *Lef1*, and *Axin2*, only occurred when osteoblasts were treated with CM derived from activated *Dkk1*-expressing T cells, whereas *Dkk1* deletion fully abolished this effect (Figures 5N–5P). Interestingly, the induction of Wnt target genes in osteoblasts cultured with CM from inactive T cells appeared blunted when *Dkk1* in the CM was absent, even though a significantly increased expression was observed for *Lef1* and *Axin2*. These data suggest that T cells deficient of *Dkk1* show less inhibitory effects on osteoblast differentiation than T cells that express DKK1. To examine whether this is a direct effect of secreted DKK1 on osteoblasts we performed co-culture experiments with CM from activated WT T cells and osteoblasts with and without the addition of a DKK1 neutralizing antibody or isotype control. Neutralization of DKK1 in CM from activated T cells did not rescue the downregulation of the osteoblast markers *Runx2*, *Osx*, *Alp*, and *Ocn* (Figures S5A–5D), implying that other factors that secreted DKK1 produced by activated T cells inhibit osteoblast differentiation.

T-cell-specific deletion of *Dkk1* protects against estrogen-deficiency-induced bone loss

To finally address whether T cells contribute to the pathogenesis of OVX-induced bone loss via their expression of DKK1, we subjected *Dkk1*$^{fl/fl}$;*Lck-Cre* mice to OVX. Estrogen withdrawal resulted in a reduced

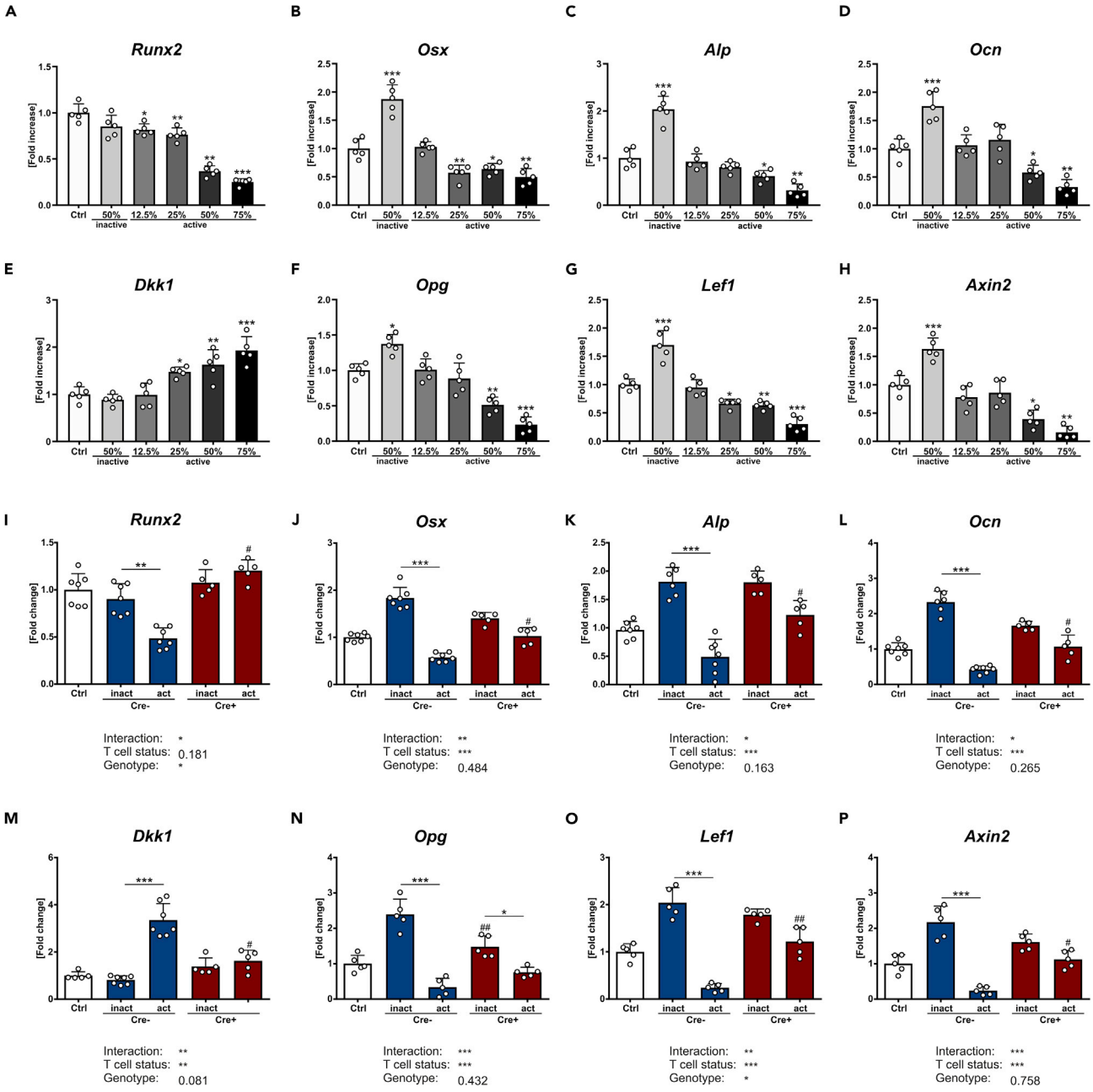

Figure 5. T cells influence osteoblast differentiation dependent on their activation status

(A–H) Primary osteoblasts from 12-week-old wild-type mice were differentiated and treated with different percentages of CM from activated or inactivated T cells for a time period of 7 days.

Gene expression analysis of the osteogenic genes (A) runt-related transcription factor 2 (*Runx2*), (B) osterix (*Osx*), (C) alkaline phosphatase (*Alp*), and (D) osteocalcin (*Ocn*), as well as Dkk1, osteoprotegerin (*Opg*), lymphoid enhancer-binding factor 1 (*Lef1*), and axin-related protein 2 (*Axin2*) from wild-type-derived primary osteoblasts was performed using real-time PCR. Primary osteoblasts from 12-week-old wild-type (Cre-positive and Cre-negative) mice were differentiated and treated with CM from activated or inactivated T cells derived from 12-week-old *Dkk1*$^{fl/fl}$*;Rosa26-ERT2-Cre* mice (Cre-positive: lack *Dkk1* expression and Cre-negative: Dkk1-expressing T cells).

(I–P) Gene expression analysis of abovementioned genes was performed using real-time PCR. Gene expression levels were normalized to *β-Actin*. Data represent the mean ± SD. n = 5–7 individual mice per group. For A–H statistical analysis was performed using Student's t test for inactive versus untreated control and one-way ANOVA for dose dependency. *p < 0.05, **p < 0.01, ***p < 0.001. For I–P statistical analysis was performed using two-way ANOVA. *p < 0.05, **p < 0.01, ***p < 0.01 versus inactive or #p < 0.05, ##p < 0.01, ###p < 0.001 versus respective Cre-negative control.

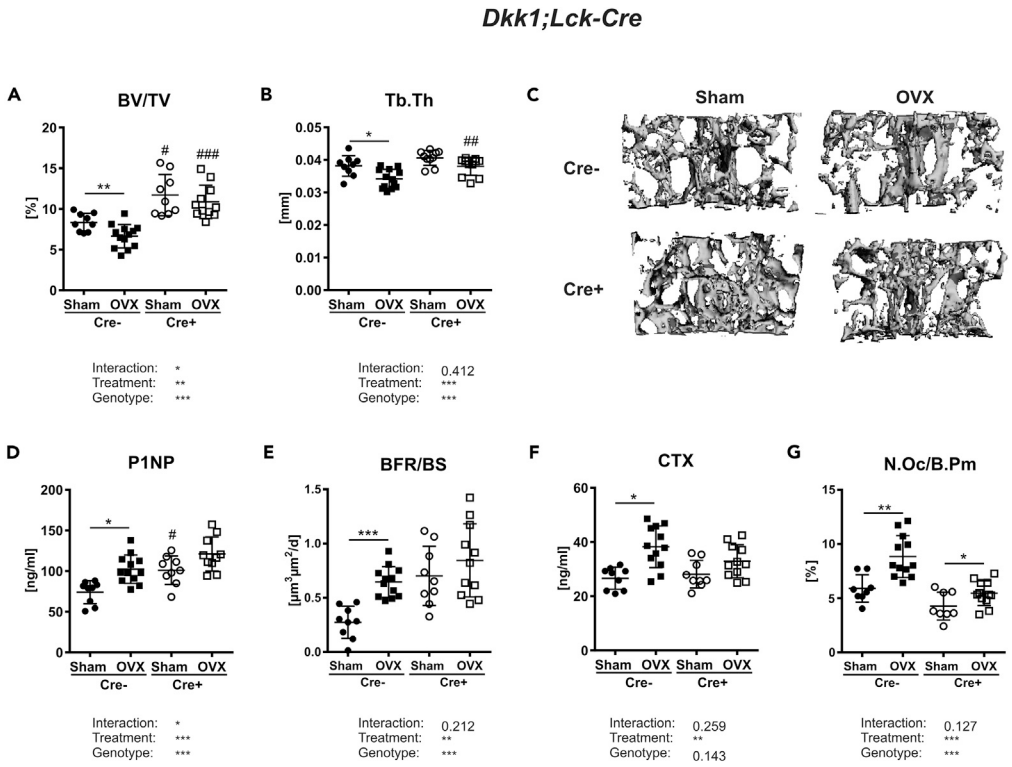

Figure 6. T-cell-specific *Dkk1* deletion protects against estrogen-deficiency-induced bone loss

The fourth vertebral body of 14-week-old female Sham operated or ovariectomized (OVX) *Dkk1*$^{fl/fl}$;*Lck-Cre* and Cre-negative control mice were analyzed by µCT.

(A and B) (A) Trabecular bone volume per total volume (BV/TV) and (B) trabecular thickness (Tb.Th) of fourth vertebral body.

(C) Representative 3D reconstruction of the analyzed fourth vertebral body.

(D–F) (D) Serum levels of the Wnt inhibitors dickkopf-1 (DKK1) and (E) bone formation marker procollagen type 1 amino-terminal propeptide (P1NP) were analyzed using commercially available ELISA. Cre− Sham, n = 9; Cre− OVX, n = 12; Cre+ Sham, n = 9; Cre+ OVX, n = 10. Histomorphometric analysis of calcein double staining was performed to determine the (F) bone formation rate/bone surface (BFR/BS).

(G) Serum levels of the bone resorption marker (G) carboxy-terminal collagen crosslinks (CTX) were measured using a commercially available ELISA.

(H) The fourth vertebral body was stained with tartrate-resistant acid phosphatase (TRAP) to determine osteoclast number per bone parameter (N.Oc/B.Pm). Cre− Sham, n = 9; Cre− OVX, n = 13; Cre+ Sham, n = 9; Cre+ OVX, n = 11. Data represent the mean ± SD. Statistical analysis was performed by the two-way ANOVA. *p < 0.05, **p < 0.01, ***p < 0.001 versus Sham or #p < 0.05, ##p < 0.01, ###p < 0.001 versus respective Cre-negative control.

bone volume (−28%), trabecular number (−12%), and trabecular thickness (−11%) in Cre− controls, whereas *Dkk1*$^{fl/fl}$;*Lck-Cre* mice did not lose a significant amount of bone mass (−7%) (Figures 6A and 6B and Table S4). Trabecular separation was only increased in Cre− control mice after OVX, but not in Cre+ mice (Table S4). Representative 3D reconstructions of the fourth vertebral body are shown in Figure 6C. Loss of DKK1 in T cells further mitigated the OVX-induced activation of $CD4^+$ and $CD8^+$ T cells (Table S5). At the skeletal level, OVX only induced *Dkk1* expression in Cre− but not Cre+ mice (Figure S6). Thus, OVX-induced changes in the bone formation parameters P1NP (+38%) and the bone formation rate (+124%) were only detected in Cre− mice, but not in Cre+ mice (Figures 6D and 6E and Table S4). Along those lines, OVX led to a reduced expression of *Lef1* and *Axin2* in bone only in control mice, whereas Cre+ mice, which already had a higher baseline expression of *Lef1* and *Axin2*, showed no suppression of those markers after OVX (Figure S1E). Furthermore, estrogen withdrawal in control mice resulted in an enhanced CTX serum level and higher number of osteoclasts, whereas these changes were blunted in T-cell-specific *Dkk1* cKO mice (Figures 6F and 6G). Although OVX induced *Rankl* expression in the bone of Cre− mice, its expression was unaltered in Cre+ mice (Figure S6). *Opg* expression was significantly higher in Cre+ mice but was not changed after OVX (Figure S6). Whether the rescue in *Dkk1*$^{fl/fl}$;*Lck-Cre* mice is directly

mediated through T-cell-derived DKK1 or indirectly due to its influence on other cells and factors needs to be examined in more detail in future studies.

DISCUSSION

Whether and how T cells contribute to estrogen-deficiency-induced bone loss remains an important topic in osteoimmunology. Several studies argue for a role of T cells in ovariectomy-induced bone loss in mice (Gao et al., 2004, 2007; Grassi et al., 2007; Li et al., 2011b; Robbie-Ryan et al., 2006; Roggia et al., 2001), whereas earlier studies failed to confirm this (Anginot et al., 2007; Lee et al., 2006). In this study, we show experimental evidence underlining a role of T cells in estrogen-deficiency-induced bone loss, however, not via the well-known effects of activated T cells on osteoclasts (Cenci et al., 2000, 2003; Roggia et al., 2001; Takayanagi, 2007) but via their inhibition of Wnt signaling in osteoblasts in a paracrine fashion.

By globally deleting DKK1 in adolescent mice, we confirmed previous studies using DKK1 inhibition strategies with monoclonal antibodies or antisense oligonucleotides (Glantschnig et al., 2011; Wang et al., 2007) and show that DKK1 is a key mediator of estrogen-deficiency-induced bone loss. However, osteogenic cells, which appear to be the main producers of circulating DKK1 (Colditz et al., 2018), were not accountable for estrogen-deficiency-induced bone loss via DKK1 production, but T cells. Mechanistically, the protection against ovariectomy-induced bone loss in global *Dkk*1 cKO mice appears to be linked to the lack of induction of bone formation, rather than inhibition of bone resorption. Even though increased bone resorption is considered one of the key mechanisms of estrogen-deficiency-induced bone loss, an increased bone formation rate, i.e. increased bone turnover, is found in a significant proportion of postmenopausal women with osteoporosis (Garnero et al., 2000; Jabbar et al., 2011; Ross et al., 2000). This high rate of bone turnover was also appreciated in our ovariectomy mouse model. As bone resorption parameters were increased in all ovariectomized mice regardless of genotype, yet, only Cre-negative control mice and osteogenic *Dkk1*-deficient mice lost a significant amount of bone, these data suggest that DKK1 does not mediate estrogen-deficiency-induced bone loss by increasing bone resorption. This was somewhat surprising considering the well-established link between Wnt signaling in osteoblasts and the subsequent regulation of the RANKL/OPG system and osteoclastogenesis. Several studies have shown that canonical Wnt/β-catenin signaling in osteoblastic cells inhibits osteoclast differentiation by increasing *Opg* and decreasing *Rankl* expression *in vitro* and *in vivo* (Glass et al., 2005; Holmen et al., 2005; Shin et al., 2005; Spencer, 2006). Intriguingly, global and T-cell-specific loss of DKK1 prevented the ovariectomy-induced increase in the RANKL/OPG ratio in bone but failed to mitigate the increase in osteoclast numbers, suggesting that mechanisms other than the RANKL/OPG system may contribute to enhanced osteoclast formation during estrogen deficiency.

Importantly, estrogen withdrawal increased systemic and even more so local bone formation in control mice, *Dkk1*$^{fl/fl}$*;Osx-Cre,* and *Dkk1*$^{fl/fl}$*;Dmp1-Cre* mice but not in global or T-cell-specific *Dkk1* cKO mice, suggesting that limiting the increase of bone formation is the primary mechanism in the prevention of ovariectomy-induced bone loss. This mechanism appears to be mediated via alterations occurring by the deficiency of DKK1 in activated T cells. In fact, co-cultures showed that activated T cells, as occurring during estrogen deficiency, expressed higher amounts of DKK1 and inhibited the expression of osteoblastic markers. This effect was limited to activated T cells, as naive T cells even increased osteoblastic gene expression. Differential effects of T cell subpopulations and/or activation states have also been observed in osteoclasts. Although Th1 and Th17 cells enhance osteoclastogenesis via their production of pro-inflammatory cytokines and RANKL, naive and regulatory T cells suppress osteoclastogenesis (John et al., 1996; Li et al., 2007b; Toraldo et al., 2003). Importantly, the negative effect of activated T cells on osteoblasts was not only found *in vitro*, but also *in vivo*, indicated by the high bone formation rate in mice lacking DKK1 specifically in T cells. Taken together, our study suggests that T cells express DKK1, as previously shown for human Foxp3^{+} T_{reg} cells (Chae et al., 2017), and that T cells can modulate osteoblast activity not only through the production of Wnt10b as previously published (Hardiman et al., 1996; Ouji et al., 2006; Terauchi et al., 2009) but also via effects mediated via DKK1. Our findings are in contradiction to other studies that showed that activated human T cells promote osteoblast differentiation (Croes et al., 2016; Rifas et al., 2003). However, in another study using mouse cells, osteoblast markers were suppressed by activated, but not resting, T cells, which is in line with our data (Young et al., 2005). Although the number of major T cell subsets and the expression of CD69 were not altered in *Dkk1*$^{fl/fl}$*;Lck-Cre* mice, *in vitro* neutralization of DKK1 had no effect on osteoblast differentiation. Therefore, we cannot rule out

whether the effect of DKK1 from T cells on bone comes directly from DKK1 or indirectly through other factors that are changed in *Dkk1*$^{fl/fl}$;*Lck-Cre* mice.

Besides elucidating the mechanisms of how T cells affect osteoblast function and bone mass, this study investigated changes in the immune cell status during estrogen deficiency, another somewhat controversially discussed topic. Our study shows that ovariectomy increases the proportion and activation of CD4+ and CD8+ T cells, whereas B cell numbers are not affected. Several studies, however, have shown that B lymphopoiesis is stimulated during estrogen deficiency (Mansoori et al., 2016; Masuzawa et al., 1994; Onal et al., 2012; Tyagi et al., 2011), whereas estrogen treatment inhibits B cell development (Erlandsson et al., 2003). Moreover, some studies suggest that B cells may contribute to ovariectomy-induced bone loss via their secretion of RANKL and other inflammatory factors (Miyaura et al., 1997). Importantly, most of the studies that found increased B cell numbers after ovariectomy analyzed B cells in the bone marrow, while we assessed the number of B cells in the spleen. In fact, our study is in line with a previous study showing an increased number of B cells in the bone marrow but not in the spleen of ovariectomized mice (Bernardi et al., 2014). Thus, estrogen deficiency may have more profound effects on B cells in the bone microenvironment: However, details about the differential regulation of B cells during estrogen deficiency need to be further delineated.

With regard to T cells, several studies show an increase in T cell numbers and activation status after estrogen withdrawal in mice (Gao et al., 2004, 2007; Grassi et al., 2007; Li et al., 2011a; Robbie-Ryan et al., 2006; Roggia et al., 2001). In addition, menopause has been shown to upregulate T cell activity and increased T cell production of cytokines (Adeel et al., 2013; D'Amelio et al., 2008), whereas hormone therapy decreases osteoclastogenic cytokine production in postmenopausal women (Rogers and Eastell, 2001). As both osteoblasts and osteoclasts have been shown to activate T cells via the secretion of cytokines and by presenting antigens (Li et al., 2010; Pacifici, 2013), these cells may contribute to T cell activation in estrogen deficiency, which is characterized by a state of high bone turnover. Furthermore, the increased T-cell-mediated secretion of TNFα has also been shown to synergize with RANKL, thereby upregulating bone resorption (Cenci et al., 2000). By suppressing the expansion of $CD4^+$ T cells and TNFα production, bone loss is prevented in ovariectomized mice (Zhang et al., 2016), further underlining the importance of T cell activation in bone loss induced by estrogen deficiency. Besides pro-inflammatory cytokines, we now also show that increased expression of DKK1 in T cells after estrogen withdrawal seems to contribute to bone loss via modulating osteoblast function, likely through indirect mechanisms. Nonetheless, additional cell types may be involved in the actions of DKK1 in ovariectomy-induced bone loss, as mice with a T-cell-specific *Dkk1* deletion still exhibited increased DKK1 serum levels after ovariectomy and a tendency of reduced bone mass, whereas global *Dkk1* deletion fully abolished bone loss.

Finally, our study shows that T cell expansion and activation due to ovariectomy was inhibited in global and T-cell-specific *Dkk1* knock-out mice, indicating that DKK1 may be an important autocrine activator of T cells during estrogen deficiency. Indeed, a critical role of the canonical Wnt pathway in T cell biology has been suggested in multiple experimental systems (Ding et al., 2008; Guo et al., 2007; vanLoosdregt et al., 2013; Xie et al., 2005). Moreover, an increasing body of evidence suggests direct immunomodulatory effects of DKK1. As such, recent studies showed that DKK1 is also present in $Foxp3^+$ T_{reg} cells, where it controls effector $CD4^+$ T cell function and is an important regulator of immunological tolerance in colitis (Chae et al., 2017). Further, numerous studies suggest that DKK1 plays a pro-inflammatory role in various diseases including asthma, parasitic or viral infection, and cancer (Chae et al., 2016; D'Amico et al., 2016; Guo et al., 2015; Malladi et al., 2016). It is important to note that besides the classical Wnt ligands and LRP receptors, DKK1 may use different types of receptors to trigger other signaling pathways. Recent studies indicate formally unknown receptors such as cytoskeleton-associated protein-4 to transmit DKK1-mediated signaling events (Kimura et al., 2016; Moon and Gough, 2016). Additional studies are required to unravel how DKK1 promotes T cell activation and proliferation under pathological conditions.

Taken together, our study highlights the importance of T cells in the control of bone mass maintenance and pathological bone remodeling in states of estrogen deficiency and suggest that dysregulations of Wnt signaling may play a critical role therein.

Limitations of the study

When considering these results, it should be noticed that our study is limited by the use of Cre-lines, which are never completely specific, as well as the use of tamoxifen, which has intrinsic effects on bone. However,

by using appropriate controls, these limitations are kept at a minimum and effects of tamoxifen were shown to be negligible as Cre-negative controls, which also received tamoxifen, showed reduced bone mass after ovariectomy. Moreover, we did not include a Dkk1$^{+/+}$;Lck-Cre-positive line as additional control. However, the similar T cell phenotype in *Dkk1$^{fl/fl}$;Rosa26-CreERT2* and *Dkk1$^{fl/fl}$;Lck-Cre* mice suggest no major effect of the *Lck-Cre* on T cells. Also, mice were ovariectomized at a relatively young age.

Resource availability

Lead contact

Further information and requests for resources and reagents should be directed to and will be fulfilled by the lead contact, Martina Rauner (martina.rauner@ukdd.de).

Materials availability

All unique/stable reagents generated in this study are available from the lead contact with a completed materials transfer agreement.

Data and code availability

No large datasets were generated within this study. Original data can be made available upon request.

METHODS

All methods can be found in the accompanying transparent methods supplemental file.

SUPPLEMENTAL INFORMATION

Supplemental information can be found online at https://doi.org/10.1016/j.isci.2021.102224.

ACKNOWLEDGMENTS

We would like to thank our technicians Tina Dybek and Ina Gloe for their excellent work. This work was supported by grants from the German Research Foundation to TDR, LCH, MR, and ST. MR was supported by the Support-the-Best Initiative of the TUD-funded through the Excellence Initiative of the German Federal and State Governments. ST was supported by the Maria Reiche program of the Medical Faculty of the Technische Universität Dresden. Graphical abstract was created with Biorender.com.

AUTHOR CONTRIBUTIONS

Study Design: JL, ST, and MR. Data collection: JL, ST, and UB. Data analysis: JL, ST, UB, and MR. Data interpretation: JL, ST, UB, TDR, CN, LCH, and MR. Drafting Manuscript: JL, LCH, and MR. Revising and approving final version of manuscript: all authors. MR takes responsibility of the integrity of the data analysis.

DECLARATION OF INTERESTS

The authors declare no competing interests.

Received: January 8, 2020
Revised: January 16, 2021
Accepted: February 19, 2021
Published: March 19, 2021

REFERENCES

Adeel, S., Singh, K., Vydareny, K.H., Kumari, M., Shah, E., Weitzmann, M.N., and Tangpricha, V. (2013). Bone loss in surgically ovariectomized premenopausal women is associated with T lymphocyte activation and thymic hypertrophy. J. Invest. Med. *61*, 1178–1183.

Ahmed, S.F., Fouda, N., and Abbas, A.A. (2013). Serum dickkopf-1 level in postmenopausal females: correlation with bone mineral density and serum biochemical markers. J. Osteoporos. *2013*, e460210.

Anginot, A., Dacquin, R., Mazzorana, M., and Jurdic, P. (2007). Lymphocytes and the Dap12 adaptor are key regulators of osteoclast activation associated with gonadal failure. PLoS One *2*, e585.

Baumann, S., Dostert, A., Novae, N., Bauer, A., Schmid, W., Fas, S.C., Krueger, A., Heinzel, T., Kirchhoff, S., Schütz, G., et al. (2005). Glucocorticoids inhibit activation-induced cell death (AICD) via direct DNA-dependent repression of the CD95 ligand gene by a glucocorticoid receptor dimer. Blood *106*, 617–625.

Bedi, B., Li, J.-Y., Tawfeek, H., Baek, K.-H., Adams, J., Vangara, S.S., Chang, M.-K., Kneissel, M., Weitzmann, M.N., and Pacifici, R. (2012). Silencing of parathyroid hormone (PTH) receptor 1 in T cells blunts the bone anabolic activity of PTH. Proc. Natl. Acad. Sci. U S A *109*, E725–E733.

Bernardi, A.I., Andersson, A., Grahnemo, L., Nurkkala-Karlsson, M., Ohlsson, C., Carlsten,

H., and Islander, U. (2014). Effects of lasofoxifene and bazedoxifene on B cell development and function. Immunity, Inflamm. Dis. *2*, 214–225.

Bhat, B.M., Allen, K.M., Liu, W., Graham, J., Morales, A., Anisowicz, A., Lam, H.S., McCauley, C., Coleburn, V., Cain, M., et al. (2007). Structure-based mutation analysis shows the importance of LRP5 β-propeller 1 in modulating Dkk1-mediated inhibition of Wnt signaling. Gene *391*, 103–112.

Burge, R., Dawson-Hughes, B., Solomon, D.H., Wong, J.B., King, A., and Tosteson, A. (2007). Incidence and economic burden of osteoporosis-related fractures in the United States, 2005-2025. J. Bone Miner. Res. *22*, 465–475.

Carow, B., Gao, Y., Coquet, J., Reilly, M., and Rottenberg, M.E. (2016). Lck -driven cre expression alters T cell development in the thymus and the frequencies and functions of peripheral T cell subsets. J. Immunol. *197*, 2261–2268.

Cenci, S., Weitzmann, M.N., Roggia, C., Namba, N., Novack, D., Woodring, J., and Pacifici, R. (2000). Estrogen deficiency induces bone loss by enhancing T-cell production of TNF-α. J. Clin. Invest. *106*, 1229–1237.

Cenci, S., Toraldo, G., Weitzmann, M.N., Roggia, C., Gao, Y., Qian, W.P., Sierra, O., and Pacifici, R. (2003). Estrogen deficiency induces bone loss by increasing T cell proliferation and lifespan through IFN-gamma-induced class II transactivator. Proc. Natl. Acad. Sci. U S A *100*, 10405–10410.

Chae, W.-J.J., Ehrlich, A.K., Chan, P.Y., Teixeira, A.M., Henegariu, O., Hao, L., Shin, J.H., Park, J.-H.H., Tang, W.H., Kim, S.-T.T., et al. (2016). The Wnt antagonist Dickkopf-1 promotes pathological type 2 cell-mediated inflammation. Immunity *44*, 246–258.

Chae, W.-J.J., Park, J.-H.H., Henegariu, O., Yilmaz, S., Hao, L., and Bothwell, A.L.M.M. (2017). Membrane-bound Dickkopf-1 in Foxp3+regulatory T cells suppresses T-cell-mediated autoimmune colitis. Immunology *152*, 265–275.

Christodoulides, C., Laudes, M., Cawthorn, W.P., Schinner, S., Soos, M., O'Rahilly, S., Sethi, J.K., and Vidal-Puig, A. (2006). The Wnt antagonist Dickkopf-1 and its receptors are coordinately regulated during early human adipogenesis. J. Cell Sci. *119*, 2613–2620.

Colditz, J., Thiele, S., Baschant, U., Garbe, A.I., Niehrs, C., Hofbauer, L.C., and Rauner, M. (2019). Osteogenic Dkk1 mediates glucocorticoid-induced, but not arthritis-induced bone loss. J. Bone Miner. Res. *34*, 1314–1323.

Colditz, J., Thiele, S., Baschant, U., Niehrs, C., Bonewald, L.F., Hofbauer, L.C., and Rauner, M. (2018). Postnatal skeletal deletion of Dickkopf-1 increases bone formation and bone volume in male and female mice, despite increased sclerostin expression. J. Bone Miner. Res. *33*, 1698–1707.

Croes, M., Öner, F.C., van Neerven, D., Sabir, E., Kruyt, M.C., Blokhuis, T.J., Dhert, W.J.A., and Alblas, J. (2016). Proinflammatory T cells and IL-17 stimulate osteoblast differentiation. Bone *84*, 262–270.

D'Amelio, P., Grimaldi, A., Di Bella, S., Brianza, S.Z.M., Cristofaro, M.A., Tamone, C., Giribaldi, G., Ulliers, D., Pescarmona, G.P., and Isaia, G. (2008). Estrogen deficiency increases osteoclastogenesis up-regulating T cells activity: a key mechanism in osteoporosis. Bone *43*, 92–100.

D'Amico, L., Mahajan, S., Capietto, A.-H., Yang, Z., Zamani, A., Ricci, B., Bumpass, D.B., Meyer, M., Su, X., Wang-Gillam, A., et al. (2016). Dickkopf-related protein 1 (Dkk1) regulates the accumulation and function of myeloid derived suppressor cells in cancer. J. Exp. Med. *213*, 827–840.

Diarra, D., Stolina, M., Polzer, K., Zwerina, J., Ominsky, M.S., Dwyer, D., Korb, A., Smolen, J., Hoffmann, M., Scheinecker, C., et al. (2007). Dickkopf-1 is a master regulator of joint remodeling. Nat. Med. *13*, 156–163.

Ding, Y., Shen, S., Lino, A.C., Curotto De Lafaille, M.A., and Lafaille, J.J. (2008). Beta-catenin stabilization extends regulatory T cell survival and induces anergy in nonregulatory T cells. Nat. Med. *14*, 162–169.

Eastell, R., O'Neill, T.W., Hofbauer, L.C., Langdahl, B., Reid, I.R., Gold, D.T., and Cummings, S.R. (2016). Postmenopausal osteoporosis. Nat. Rev. Dis. Prim. *2*, e16069.

Erlandsson, M.C., Jonsson, C.A., Islander, U., Ohlsson, C., and Carlsten, H. (2003). Oestrogen receptor specificity in oestradiol-mediated effects on B lymphopoiesis and immunoglobulin production in male mice. Immunology *108*, 346–351.

Fujiwara, Y., Piemontese, M., Liu, Y., Thostenson, J.D., Xiong, J., and O'Brien, C.A. (2016). RANKL (Receptor Activator of NFκB Ligand) produced by osteocytes is required for the increase in B cells and bone loss caused by estrogen deficiency in mice. J. Biol. Chem. *291*, 24838–24850.

Gao, Y., Qian, W.-P.W.-P., Dark, K., Toraldo, G., Lin, A.S.P., Guldberg, R.E., Flavell, R.A., Weitzmann, M.N., and Pacifici, R. (2004). Estrogen prevents bone loss through transforming growth factor beta signaling in T cells. Proc. Natl. Acad. Sci. *101*, 16618–16623.

Gao, Y., Grassi, F., Ryan, M.R., Terauchi, M., Page, K., Yang, X., Weitzmann, M.N., and Pacifici, R. (2007). IFN-γ stimulates osteoclast formation and bone loss in vivo via antigen-driven T cell activation. J. Clin. Invest. *117*, 122–132.

Garcia-Perez, M.A., Noguera, I., Hermenegildo, C., Martínez-Romero, A., Tarín, J.J., and Cano, A. (2005). Alterations in the phenotype and function of immune cells in ovariectomy-induced osteopenic mice. Hum. Reprod. *21*, 880–887.

Garnero, P., Sornay-Rendu, E., Claustrat, B., and Delmas, P.D. (2000). Biochemical markers of bone turnover, endogenous hormones and the risk of fractures in postmenopausal women: the OFELY study. J. Bone Miner. Res. *15*, 1526–1536.

Glantschnig, H., Scott, K., Hampton, R., Wei, N., McCracken, P., Nantermet, P., Zhao, J.Z., Vitelli, S., Huang, L., Haytko, P., et al. (2011). A rate-limiting role for Dickkopf-1 in bone formation and the remediation of bone loss in mouse and primate models of postmenopausal osteoporosis by an experimental therapeutic antibody. J. Pharmacol. Exp. Ther. *338*, 568–578.

Glass, D.A., Bialek, P., Ahn, J.D., Starbuck, M., Patel, M.S., Clevers, H., Taketo, M.M., Long, F., McMahon, A.P., Lang, R.A., et al. (2005). Canonical Wnt signaling in differentiated osteoblasts controls osteoclast differentiation. Dev. Cell *8*, 751–764.

Grassi, F., Tell, G., Robbie-Ryan, M., Gao, Y., Terauchi, M., Yang, X., Romanello, M., Jones, D.P., Weitzmann, M.N., and Pacifici, R. (2007). Oxidative stress causes bone loss in estrogen-deficient mice through enhanced bone marrow dendritic cell activation. Proc. Natl. Acad. Sci. *104*, 15087–15092.

Guo, Y., Mishra, A., Howland, E., Zhao, C., Shukla, D., Weng, T., and Liu, L. (2015). Platelet-derived Wnt antagonist Dickkopf-1 is implicated in ICAM-1/VCAM-1-mediated neutrophilic acute lung inflammation. Blood *126*, 2220–2229.

Guo, Z., Dose, M., Kovalovsky, D., Chang, R., O'Neil, J., Look, A.T., Von Boehmer, H., Khazaie, K., and Gounari, F. (2007). β-catenin stabilization stalls the transition from double-positive to single-positive stage and predisposes thymocytes to malignant transformation. Blood *109*, 5463–5472.

Hardiman, G., Albright, S., Tsunoda, J.I., McClanahan, T., and Lee, F. (1996). The mouse Wnt-10B gene isolated from helper T cells is widely expressed and a possible oncogene in BR6 mouse mammary tumorigenesis. Gene *172*, 199–205.

Hernlund, E., Svedbom, A., Ivergård, M., Compston, J., Cooper, C., Stenmark, J., McCloskey, E.V., Jönsson, B., and Kanis, J.A. (2013). Osteoporosis in the European union: medical management, epidemiology and economic burden: a report prepared in collaboration with the international osteoporosis foundation (IOF) and the European federation of pharmaceutical industry associations (EFPIA). Arch. Osteoporos. *8*, 1–115.

Holmen, S.L., Zylstra, C.R., Mukherjee, A., Sigler, R.E., Faugere, M.C., Bouxsein, M.L., Deng, L., Clemens, T.L., and Williams, B.O. (2005). Essential role of beta-catenin in postnatal bone acquisition. J. Biol. Chem. *280*, 21162–21168.

Jabbar, S., Drury, J., Fordham, J.N., Datta, H.K., Francis, R.M., and Tuck, S.P. (2011). Osteoprotegerin, RANKL and bone turnover in postmenopausal osteoporosis. J. Clin. Pathol. *64*, 354–357.

John, V., Hock, J.M., Short, L.L., Glasebrook, A.L., and Galvin, R.J. (1996). A role for CD8+ T lymphocytes in osteoclast differentiation in vitro. Endocrinology *137*, 2457–2463.

Kimura, H., Fumoto, K., Shojima, K., Nojima, S., Osugi, Y., Tomihara, H., Eguchi, H., Shintani, Y., Endo, H., Inoue, M., et al. (2016). CKAP4 is a Dickkopf1 receptor and is involved in tumor progression. J. Clin. Invest. *126*, 2689–2705.

Lee, S.-K.K., Kadono, Y., Okada, F., Jacquin, C., Koczon-Jaremko, B., Gronowicz, G., Adams, D.J., Aguila, H.L., Choi, Y., and Lorenzo, J.A. (2006). T lymphocyte-deficient mice lose trabecular bone

mass with ovariectomy. J. Bone Miner. Res. *21*, 1704–1712.

Li, H., Hong, S., Qian, J., Zheng, Y., Yang, J., and Yi, Q. (2010). Cross talk between the bone and immune systems: osteoclasts function as antigen-presenting cells and activate CD4+and CD8+T cells. Blood *116*, 210–217.

Li, J.-Y., Tawfeek, H., Bedi, B., Yang, X., Adams, J., Gao, K.Y., Zayzafoon, M., Weitzmann, M.N., and Pacifici, R. (2011a). Ovariectomy disregulates osteoblast and osteoclast formation through the T-cell receptor CD40 ligand. Proc. Natl. Acad. Sci. U S A *108*, 768–773.

Li, J., Sarosi, I., Cattley, R.C., Pretorius, J., Asuncion, F., Grisanti, M., Morony, S., Adamu, S., Geng, Z., Qiu, W., et al. (2006). Dkk1-mediated inhibition of Wnt signaling in bone results in osteopenia. Bone *39*, 754–766.

Li, X., Grisanti, M., Fan, W., Asuncion, F.J., Tan, H.L., Dwyer, D., Han, C.Y., Yu, L., Lee, J., Lee, E., et al. (2011b). Dickkopf-1 regulates bone formation in young growing rodents and upon traumatic injury. J. Bone Miner. Res. *26*, 2610–2612.

Li, Y., Li, A., Yang, X., and Weitzmann, M.N. (2007a). Ovariectomy-induced bone loss occurs independently of B cells. J. Cell. Biochem. *100*, 1370–1375.

Li, Y., Toraldo, G., Li, A., Yang, X., Zhang, H., Qian, W.P., and Weitzmann, M.N. (2007b). B cells and T cells are critical for the preservation of bone homeostasis and attainment of peak bone mass in vivo. Blood *109*, 3839–3848.

Malladi, S., MacAlinao, D.G., Jin, X., He, L., Basnet, H., Zou, Y., De Stanchina, E., and Massagué, J. (2016). Metastatic latency and immune evasion through autocrine inhibition of WNT. Cell *165*, 45–60.

Mansoori, M.N., Shukla, P., Kakaji, M., Tyagi, A.M., Srivastava, K., Shukla, M., Dixit, M., Kureel, J., Gupta, S., and Singh, D. (2016). IL-18BP is decreased in osteoporotic women: prevents Inflammasome mediated IL-18 activation and reduces Th17 differentiation. Sci. Rep. *6*, 33680.

Mao, B., Wu, W., Li, Y., Hoppe, D., Stannek, P., Glinka, A., and Niehrs, C. (2001). LDL-receptor-related protein 6 is a receptor for Dickkopf proteins. Nature *411*, 321–325.

Mao, B., Wu, W., Davidson, G., Marhold, J., Li, M., Mechler, B.M., Dellus, H., Hoppe, D., Stannek, P., Walter, C., et al. (2002). Kremen proteins are Dickkopf receptors that regulate Wnt/β-catenin signalling. Nature *417*, 664–667.

Masuzawa, T., Miyaura, C., Onoe, Y., Kusano, K., Ohta, H., Nozawa, S., and Suda, T. (1994). Estrogen deficiency stimulates B lymphopoiesis in mouse bone marrow. J. Clin. Invest. *94*, 1090–1097.

Miyaura, C., Onoe, Y., Inada, M., Maki, K., Ikuta, K., Ito, M., and Suda, T. (1997). Increased B-lymphopoiesis by interleukin 7 induces bone loss in mice with intact ovarian function: similarity to estrogen deficiency. Proc. Natl. Acad. Sci. U S A *94*, 9360–9365.

Moon, R.T., and Gough, N.R. (2016). Beyond canonical: the Wnt and β-catenin story. Sci. Signal. *9*, 1–2.

Morvan, F., Boulukos, K., Clément-Lacroix, P., Roman, S.R., Suc-Royer, I., Vayssière, B., Ammann, P., Martin, P., Pinho, S., Pognonec, P., et al. (2006). Deletion of a single allele of the Dkk1 gene leads to an increase in bone formation and bone mass. J. Bone Miner. Res. *21*, 934–945.

Onal, M., Xiong, J., Chen, X., Thostenson, J.D., Almeida, M., Manolagas, S.C., and O'Brien, C.A. (2012). Receptor activator of nuclear factor κB ligand (RANKL) protein expression by B lymphocytes contributes to ovariectomy-induced bone loss. J. Biol. Chem. *287*, 29851–29860.

Ouji, Y., Yoshikawa, M., Shiroi, A., and Ishizaka, S. (2006). Wnt-10b secreted from lymphocytes promotes differentiation of skin epithelial cells. Biochem. Biophys. Res. Commun. *342*, 1063–1069.

Pacifici, R. (2012). Role of T cells in ovariectomy induced bone loss- revisited. J. Bone Miner. Res. *27*, 231–239.

Pacifici, R. (2013). Osteoimmunology and its implications for transplantation. Am. J. Transpl. *13*, 2245–2254.

Pietilä, I., Ellwanger, K., Railo, A., Jokela, T., Barrantes, I.del B., Shan, J., Niehrs, C., and Vainio, S.J. (2011). Secreted Wnt antagonist Dickkopf-1 controls kidney papilla development coordinated by Wnt-7b signalling. Dev. Biol. *353*, 50–60.

Pozzi, S., Fulciniti, M., Yan, H., Vallet, S., Eda, H., Patel, K., Santo, L., Cirstea, D., Hideshima, T., Schirtzinge, L., et al. (2013). In vivo and in vitro effects of a novel anti-Dkk1 neutralizing antibody in multiple myeloma. Bone *53*, 487–496.

Qiu, X., Gui, Y., Zhang, N., Xu, Y., Li, D., and Wang, L. (2016). Effects of Bu-Shen-Ning-Xin Decoction on immune cells of the spleen and bone marrow in ovariectomized mice. Biosci. Trends *10*, 400–409.

Rachner, T.D., Khosla, S., and Hofbauer, L.C. (2011). Osteoporosis: now and the future. Lancet *377*, 1276–1287.

Rachner, T.D., Göbel, A., Thiele, S., Rauner, M., Benad-Mehner, P., Hadji, P., Bauer, T., Muders, M.H., Baretton, G.B., Jakob, F., et al. (2014). Dickkopf-1 is regulated by the mevalonate pathway in breast cancer. Breast Cancer Res. *16*, R20.

Rauner, M., Thiele, S., Sinningen, K., Winzer, M., Salbach-Hirsch, J., Gloe, I., Peschke, K., Haegeman, G., Tuckermann, J.P., and Hofbauer, L.C. (2013). Effects of the selective glucocorticoid receptor modulator compound A on bone metabolism and inflammation in male mice with collagen-induced arthritis. Endocrinology *154*, 3719–3728.

Rifas, L., Arackal, S., and Weitzmann, M.N. (2003). Inflammatory T cells rapidly induce differentiation of human bone marrow stromal cells into mature osteoblasts. J. Cell. Biochem. *88*, 650–659.

Robbie-Ryan, M., Pacifici, R., and Weitzmann, M.N. (2006). IL-7 drives T cell-mediated bone loss following ovariectomy. Ann. N. Y. Acad. Sci. *1068*, 348–351.

Rogers, A., and Eastell, R. (2001). The effect of 17β-estradiol on production of cytokines in cultures of peripheral blood. Bone *29*, 30–34.

Roggia, C., Gao, Y., Cenci, S., Weitzmann, M.N., Toraldo, G., Isaia, G., and Pacifici, R. (2001). Up-regulation of TNF-producing T cells in the bone marrow: a key mechanism by which estrogen deficiency induces bone loss in vivo. Proc. Natl. Acad. Sci. *98*, 13960–13965.

Ross, P.D., Kress, B.C., Parson, R.E., Wasnich, R.D., Armour, K.A., and Mizrahi, I.A. (2000). Serum bone alkaline phosphatase and calcaneus bone density predict fractures: a prospective study. Osteoporos. Int. *11*, 76–82.

Shin, C.S., Her, S.J., Kim, J.G.J.A., Kim, D.H., Kim, S.W.S.Y., Kim, S.W.S.Y., Kim, H.S., Park, K.H., Kim, J.G.J.A., Kitazawa, R., et al. (2005). Dominant negative N-cadherin inhibits osteoclast differentiation by interfering with β-catenin regulation of RANKL, independent of cell-cell adhesion. J. Bone Miner. Res. *20*, 2200–2212.

Spencer, G.J. (2006). Wnt signalling in osteoblasts regulates expression of the receptor activator of NF B ligand and inhibits osteoclastogenesis in vitro. J. Cell Sci. *119*, 1283–1296.

van Staa, T.P., Dennison, E.M., Leufkens, H.G.G.M., Cooper, C., Baron, J., Karagas, M., Barrett, J., Kniffin, W., Malenka, D., Mayor, M., et al. (2001). Epidemiology of fractures in england and wales. Bone *29*, 517–522.

Takayanagi, H. (2007). Osteoimmunology: Shared Mechanisms and Crosstalk between the Immune and Bone Systems.

Terauchi, M., Li, J.Y., Bedi, B., Baek, K.H., Tawfeek, H., Galley, S., Gilbert, L., Nanes, M.S., Zayzafoon, M., Guldberg, R., et al. (2009). T lymphocytes amplify the anabolic activity of parathyroid hormone through Wnt10b signaling. Cell Metab. *10*, 229–240.

Tian, E., Zhan, F., Walker, R., Rasmussen, E., Ma, Y., Barlogie, B., and Shaugnessey, J.D. (2003). The role of the wnt-signalling antagonist DKK1 in the development of osteolytic lesions in multiple myeloma. N. Engl. J. Med. *349*, 2438–2494.

Tian, J., Xu, X.J., Shen, L., Yang, Y.P., Zhu, R., Shuai, B., Zhu, X.W., Li, C.G., Ma, C., and Lv, L. (2015). Association of serum Dkk-1 levels with β-catenin in patients with postmenopausal osteoporosis. J. Huazhong Univ. Sci. Technolog. Med. Sci. *35*, 212–218.

Toraldo, G., Roggia, C., Qian, W.-P., Pacifici, R., and Weitzmann, M.N. (2003). IL-7 induces bone loss in vivo by induction of receptor activator of nuclear factor kappa B ligand and tumor necrosis factor alpha from T cells. Proc. Natl. Acad. Sci. U S A *100*, 125–130.

Tyagi, A.M., Srivastava, K., Sharan, K., Yadav, D., Maurya, R., and Singh, D. (2011). Daidzein prevents the increase in CD4+CD28null T cells and B lymphopoesis in ovariectomized mice: a key mechanism for anti-osteoclastogenic effect. PLoS One *6*, e21216.

US Department of Health and Human Services (2004). Bone health and osteoporosis: a report of the Surgeon General. Off. Surg. Gen. 1–404.

vanLoosdregt, J., Fleskens, V., Tiemessen, M.M., Mokry, M., VanBoxtel, R., Meerding, J., Pals, C.E.G.M., Kurek, D., Baert, M.R.M., Delemarre, E.M., et al. (2013). Canonical Wnt signaling negatively modulates regulatory T cell function. Immunity *39*, 298–310.

Wang, F.S., Ko, J.Y., Lin, C.L., Wu, H.L., Ke, H.J., and Tai, P.J. (2007). Knocking down dickkopf-1 alleviates estrogen deficiency induction of bone loss. A histomorphological study in ovariectomized rats. Bone *40*, 485–492.

Wang, F.S., Ko, J.Y., Yeh, D.W., Ke, H.C., and Wu, H.L. (2008). Modulation of Dickkopf-1 attenuates glucocorticoid induction of osteoblast apoptosis, adipocytic differentiation, and bone mass loss. Endocrinology *149*, 1793–1801.

Xie, H., Huang, Z., Sadim, M.S., and Sun, Z. (2005). Stabilized beta-catenin extends thymocyte survival by up-regulating Bcl-xL. J. Immunol. *175*, 7981–7988.

Young, N., Mikhalkevich, N., Yan, Y., Chen, D., and Zheng, W. (2005). Differential regulation of osteoblast activity by Th cell subsets mediated by parathyroid hormone and IFN-γ. J. Immunol. *175*, 8287–8295.

Zhang, N., Gui, Y., Qiu, X., Tang, W., Li, L., Gober, H.-J., Li, D., and Wang, L. (2016). DHEA prevents bone loss by suppressing the expansion of CD4(+) T cells and TNFa production in the OVX-mouse model for postmenopausal osteoporosis. Biosci. Trends *10*, 277–287.

Ziegler, S.F., Ramsdell, F., and Alderson, M.R. (1994). The activation antigen CD69. Stem Cells *12*, 456–465.

iScience, Volume *24*

Supplemental information

Mice lacking DKK1 in T cells exhibit high bone mass and are protected from estrogen-deficiency-induced bone loss

Juliane Lehmann, Sylvia Thiele, Ulrike Baschant, Tilman D. Rachner, Christof Niehrs, Lorenz C. Hofbauer, and Martina Rauner

Transparent Methods

STAR★Methods

Lead Contact and Materials Availability

Further information and requests for resources and reagents should be directed to and will be fulfilled by the Lead Contact, Martina Rauner (martina.rauner@ukdd.de). This study did not generate new unique reagents.

Experimental Model and Subject Details

For global *Dkk1* deletion tamoxifen-inducible global *Dkk1* knock-out mice (*Dkk1*$^{fl/fl}$*;Rosa26-CreERT2*) were generated 28 (Colditz et al., 2018). At the age of seven weeks male and female *Dkk1*$^{fl/fl}$*;Rosa26-CreERT2*-positive and -negative control mice were injected with 100 µl tamoxifen (10 g/l, Sigma, Germany) for 5 consecutive days to induce global deletion of *Dkk1*. For cell-specific deletion of *Dkk1* in osteogenic cells, doxycycline-repressible *Dkk1*$^{fl/fl}$*;Osx-Cre* (osteoprogenitor-specific) and constitutive *Dkk1*$^{fl/fl}$*;Dmp1-Cre* (osteocyte-specific) transgenic mouse lines were generated (Colditz et al., 2018). *Dkk1*$^{fl/fl}$*;Osx-Cre* breeding pairs received doxycycline in their drinking water (10 mg/ml in a 3% sucrose solution) *ad libitum* to repress Cre activity during embryogenesis. *Dkk1*$^{fl/fl}$*;Osx-Cre* offspring received doxycycline-drinking water until the age of five weeks. *Dkk1*$^{fl/fl}$ mice (*Dkk1*$^{fl/fl}$) 27(Pietilä et al., 2011) in which exon 1 and 2 are flanked by *loxP* sites were crossed with *Lck-Cre* mice 86 (Baschant et al., 2011) to generate T cell-specific *Dkk1* knock-out mice (*Dkk1*$^{fl/fl}$*;Lck-Cre*). Respective Cre-negative littermates were used as controls. Ly5.1 mice (Jackson Laboratory, USA) were used for T cell transfer experiments. All mice were routinely genotyped and recombination of *Dkk1* deletion in different organs was investigated. Breeding of the mouse lines was approved by the Landesdirektion Sachsen.

Method Details

In vivo experiments

All animal procedures were approved by the institutional animal care committee of the TU Dresden and the Landesdirektion Sachsen. All mice were fed a standard diet with water *ad libitum* and were kept in groups of 4 animals per cage. Mice were exposed to a 12 h light/dark cycle and an air-conditioned room at 23°C (no specific pathogen-free room). Enrichment was provided in forms of cardboard houses and bedding material. Mice were randomly assigned to treatment groups and the subsequent analyses were performed in a blinded-fashion.

Bone phenotyping: Phenotype analysis of male and female *Dkk1$^{fl/fl}$;Lck-Cre* mice was performed at an age of 12 weeks . Each group consisted of 8-11 mice.

Ovariectomy: Female 10-week-old *Dkk1$^{fl/fl}$;Rosa26-CreERT2*, *Dkk1$^{fl/fl}$;Osx-Cre*, *Dkk1$^{fl/fl}$;Dmp1-Cre*, and *Dkk1$^{fl/fl}$;Lck-Cre* mice and their respective Cre- controls were bilaterally ovariectomized or sham operated. After four weeks, mice were sacrificed for further analyses. Each group consisted of 8-16 mice.

T cell transfer: T cells were isolated from the spleen of 12-week-old Ly5.1 mice using the Pan T Cell Isolation Kit II (Miltenyi Biotec, Germany). Five or ten million T cells were transplanted via retro-orbital injection into *Dkk1$^{fl/fl}$;Lck-Cre* and littermate control mice. After three weeks bone parameters were assessed.

Micro-CT

Bone microarchitecture was analyzed *ex vivo* using the vivaCT40 (Scanco Medical, Switzerland). The femur and the fourth lumbar vertebra were imaged at a resolution of 10.5 µm with a X-ray energy of 70 kVp, 114 mA, and an integration time of 200 ms. The trabecular bone in the femur was assessed in the metaphysis 20 slices below the growth plate using 100 slices. In the vertebral bone, 100 slices were measured between both growth plates. The

cortical bone was determined in the femoral midshaft (100 slices). Pre-defined scripts from Scanco were used for the evaluation.

Bone histomorphometry

Mice were injected with 20 mg/kg calcein (Sigma-Aldrich, Germany) five and two days before sacrifice. Dynamic bone histomorphometry was performed as described previously 87 (Rauner et al.). Briefly, the third lumbar vertebra and the tibia were fixed in 4% PBS-buffered paraformaldehyde and dehydrated in an ascending ethanol series. Subsequently, bones were embedded in methacrylate and cut into 7 µm sections to assess the fluorescent calcein labels. Unstained sections were analyzed using fluorescence microscopy to determine the mineralized surface/bone surface (MS/BS), the mineral apposition rate (MAR), and the bone formation rate/bone surface (BFR/BS).

For tartrate-resistant acid phosphatase (TRAP) staining the femur and fourth lumbar vertebra were decalcified for one week using Osteosoft (Merck, Germany), dehydrated, and embedded into paraffin. TRAP staining was performed on 4 µm sections to assess the number of osteoblasts per bone perimeter (N.Ob/B.Pm), the number of osteoclasts per bone perimeter (N.Oc/B.Pm), and the number of osteocytes per bone area (N.Ot/B.Ar). Bone sections were analyzed using the Osteomeasure software (Osteometrics, USA) following international standards 88 (Dempster et al., 2013).

Cell culture

T cells were isolated from the spleen of 12-week-old WT, *Dkk1$^{fl/fl}$;Rosa26-CreERT2* or control mice using the Pan T Cell Isolation Kit II (Miltenyi Biotec, Germany). At the age of seven weeks, Dkk1 deletion was induced in *Dkk1$^{fl/fl}$;Rosa26-CreERT2*-positive and -negative mice using tamoxifen. T cells were cultured at 1x10^6 cells/ml in 24-well plates coated with murine anti-CD3 (1 µg/ml, clone 145-2C11, 1XE, Invitrogen, Germany) for activation, or cultured on uncoated wells for 3 days (inactive T cells). To obtain conditioned medium (CM), cell suspensions were harvested, centrifuged, and the supernatant was collected for storage at -

80 °C until use. To assess *Dkk1* expression in inactive and active T cells, RNA was isolated after 3 days of culture.

Co-culture of osteoblasts and T cell-derived CM was started when osteoblasts reached 70% confluence. Primary osteoblasts were differentiated from the bone marrow of WT mice using standard osteogenic medium in DMEM with 10% FCS, 1% penicillin/streptomycin (Life Technologies, Germany), 100 µM ascorbate phosphate, and 5 mM β-glycerol phosphate. The T cell CM was added to the osteoblasts at different concentrations (12.5–75%) and fresh CM was added at each medium change (two independent experiments with 3 n each). In osteogenic differentiation medium, the concentration of osteogenic stimuli was corrected for the total volume of medium. After 7 days RNA from primary osteoblasts was isolated. For DKK1 neutralizing experiments, 10 µg/ml human/mouse DKK-1 neutralizing antibody and isotype control antibody (both R&D Systems, Germany) were added to the medium and cells were differentiated for 7 days.

To obtain osteoclasts, bone marrow cells from wild-type C57BL/6 mice were isolated. Briefly femora and tibiae of each mouse were flushed through a 100 µm Nylon cell strainer with approximately 8 ml Modified Minimum Essential Medium (Alpha Medium) supplemented with 10% FCS and 1% penicillin/streptomycin, and 1 mM L-alanyl-L-glutamine (basal medium) using a 26G syringe. Cells were centrifuged for 5 min at 500 g and cell pellet was resuspended in 1 ml medium. Afterwards cells were counted and $1x10^6$ cells per cm^2 were seeded on 6-well plates. For the first 48 h basal medium was supplemented with 25 ng M-CSF. Afterwards osteoclast differentiation was induced by simultaneously treating the cells with 25 ng M-CSF and 50 ng RANKL for 7 days. After 7 days of culture, RNA was isolated using the High Pure RNA isolation kit (Promega, Madison, WI, USA).

To obtain primary macrophages, femora and tibiae of wild-type C57BL/6 mice were flushed using Roswell Park Memorial Institute (RPMI) 1640 medium supplemented with 10% FCS, 2 mM L-alanyl-L-glutamine and 1% penicillin/streptomycin (lymphocyte medium) as described above. After centrifugation for 5 min at 500 g, cells were resuspended in 1 ml lymphocyte medium supplemented with 30% L929 conditioned media (macrophage medium). For cell

culture $1x10^6$ cells per cm^2 were seeded on 6-well plates. After 24 h 1 ml fresh macrophage medium was added. At day 4 of cell culture, cells were washed twice with PBS and fresh macrophage medium was added. This step was repeated on day 6. After 7 days of culture, RNA was isolated using the peqGOLD TriFast™ isolation kit.

B cells were isolated from the spleen of 12-week-old WT mice. After the cell number was determined, B cells were sorted using Dynabeads (Invitrogen, Germany). For that, cells were stained with anti-CD45R-biotin (1:100) for 20 min at 4°C in the dark. After incubation cells were washed and the suspension was transferred into a new 2 ml reaction tube. Then 50 µl of Anti-Biotin Dynabeads per 10^7 total cells were added to the cell suspension and incubated for 30 min at 4°C with gentle rotation. Tubes were placed in a magnet for 2 min and the supernatant was carefully aspirated. After removing the tubes from the magnet, cells were resuspended in 1 ml MACS buffer, and put back in the magnet for another 2 min. Once supernatant was removed, cell pellet was stored at -80°C until RNA isolation. After 7 days of culture, RNA was isolated using the peqGOLD TriFast™ isolation kit (Promega, Madison, WI, USA)).

Flow cytometry

The right femur and the spleen were dissected and cells were isolated and filtered through a 100 µm cell strainer. Total cell number was counted, cells were blocked with anti-rat IgG and CD16/CD32, and subsequently stained with anti-CD11b-PE (1:500), anti-CD45-PE-Cy7 (1:200), and anti-Gr1-A700 (1:100) for bone marrow cells or with anti-CD45R-FITC (1:500), anti-CD3-APC (1:200), anti-CD4-PE-Cy7 (1:200), anti-CD8-A700 (1:200) and anti-CD69-PECy5 (1:100) for splenic cells for 40 minutes at 4°C in the dark. For analysis of naïve T cells, splenic cells were stained with anti-CD44-PE (1:200), anti-CD62L-APC (1:200), anti-TCRβ-APC (1:200) and anti-CD4-eF450 (1:200). Regulatory T cells were analyzed by staining for the expression of surface markers with anti-CD4-FITC (1:100), anti-CD25-PE (1:300) and, after fixation and permeabilization with intra-nuclear staining for FoxP3 using anti-FoxP3-APC (1:400) and the FOXP3 Fix/Perm Buffer Set (eBiosciences, Germany).

Thereafter, cells were washed twice with PBS and analyzed with the BD LSR II flow cytometer (BD Biosciences, San Jose, CA, USA) and the FlowJo vX software (Tree Star Inc., Ashland, OR, USA). Thymic cells were analyzed by dissecting the thymus and isolating the cells through a 100 µM cell strainer. Subsequently, total cell number was counted, cells were blocked with anti CD16/CD32 and stained with anti-CD4-PerCPCy5.5 (1:500) and anti-CD8-APC (1:300) for 40 minutes at 4°C in the dark.

For intracellular staining of DKK1, the FOXP3 Fix/Perm Buffer Set (Biolegend, Germany) was used according to protocol. After cells were fixed and permeabilized, cells were stained with the primary DKK1 biotinylated antibody (BAM1765, R&D Systems, Germany; 1:100) for 40 min at 4°C. Cells were washed twice and then stained with the secondary antibody streptavidine-Fluor450 (1:200) for 20 min at 4°C. After washing the cells they were analyzed using the LSR II and BD Diva software (BD Bioscience).

Luciferase-based reporter assays

A TCF/LEF-reporter assay (Qiagen) was done using the murine myoblast C2C12 cell line, which is commonly used to study BMP and Wnt signaling. These cells were seeded at a concentration of 1.5×10^4 cells per well in 48-well plates and were cultured in DMEM medium with 10% fetal bovine serum 1% Penicillin/Streptomycin, and transfected with the Signal TCF/LEF Reporter (CCS-018L, Qiagen, Hilden, Germany) to assess the activation of the TCF/LCF Wnt promotor. Briefly, 123 ng/cm^2 of the promotor construct was transfected using the FuGENE HD Transfection Reagent (Promega, Madison, WI, USA) according to the manufacturer's protocols. After 24 h, C2C12 cells were treated with or without Wnt3a-containing L-cell medium and/or CM from inactive or active T cells. Luciferase activity was assayed 48 h post treatment using the Dual Luciferase Reporter Assay kit (Promega, Madison, WI, USA) as instructed by the manufacturer.

Serum analysis

Blood was taken via heart punctuation of anaesthetized mice and serum was collected after

10 minutes centrifugation at 400 g. DKK1, C-terminal telopeptide (CTX), tartrate-resistant acid phosphatase form 5b (TRAP5b) and type 1 procollagen amino-terminal-propeptide (P1NP) were measured using an immunoassay kit (DKK1: R&D Systems, USA; CTX, TRAP5b and P1NP: Immundiagnostik Systems, Germany) according to the manufacturer's protocols. Samples were diluted according to protocol.

RNA isolation, RT, and real-time PCR

RNA from cell cultures was isolated using the High Pure RNA Isolation Kit (Roche) and RNA from the bones of mice was isolated by crushing flushed bones (femur and tibia) in liquid nitrogen and collecting the bone powder in Trifast (Peqlab, Germany). Five-hundred ng RNA were reverse transcribed using Superscript II (Invitrogen, Germany) und subsequently used for SYBR green-based real-time PCR analysis using a standard protocol (Life Technologies). The primer sequences were: β-actin s: GATCTGGCACCACACCTTCT, β-actin as: GGGGTGTTGAAGGTCTCAAA; Alp s: CTACTTGTGTGGCGTGAAGG, Alp as: CTGGTGGCATCTCGTTATCC; Axin2 s: GCAGTGATGGAGGAAAATGC, Axin2 as: ATTCAAGGTGGGGAGGTAGC; Dkk1 s: GCCTCCGATCATCAGACGGT, Dkk1 as: GCAGGTGTGGAGCCTAGAAG; Lef1 s: CAAATAAAGTGCCCGTGGTG, Lef1 as: TCGTCGCTGTAGGTGATGAG; Ocn s: GCGCTCTGTCTCTCTGACCT, Ocn as: ACCTTATTGCCCTCCTGCTT; Opg s: CCTTGCCCTGACCACTCTTA, Opg as: ACACTGGGCTGCAATACACA; Osx s: CTTCCCAATCCTATTTGCCGTTT, Osx as: CGGCCAGGTTACTAACACCAATCT; Rankl s: CCGAGACTACGGCAAGTACC, Rankl as: GCGCTCGAAAGTACAGGAAC; Runx2 s: CCCAGCCACCTTTACCTACA, Runx2 as: TATGGAGTGCTGCTGGTCTG. The results were calculated using the ΔΔCT method and are presented in x-fold increase relative to ***β-actin*** mRNA levels.

<u>Quantification and Statistical Analysis</u>

Data are presented as mean ± standard deviation (SD) and P values of < 0.05 were considered statistically significant. Graphs and statistics were prepared using GraphPad

Prism 7.0 software. For examination of the effect of *Dkk1* deletion and estrogen deficiency and to discover two-way interactions, a two-way factorial Analysis of variance (ANOVA) was carried out. To investigate the dose-dependency in our T cell co-culture one-way ANOVA was performed. For examination of the effect of *Dkk1* deletion on osteoblast differentiation a two-way factorial ANOVA was carried out. To analyze the effect of T cell specific *Dkk1* deletion on bone a Student's t-test was performed. Furthermore, the *Kolmogorov-Smirnov normality test* was used to examine if variables are normally distributed.

Supplementary Figures

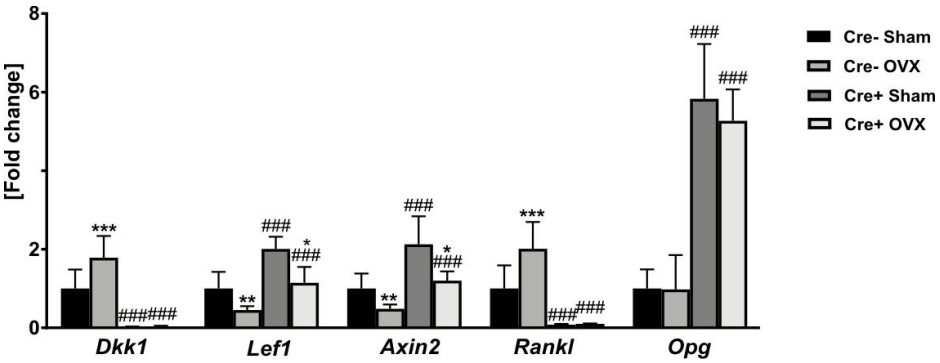

Figure S1. Global *Dkk1* cKO mice show altered Wnt signaling as well as *Rankl/Opg* ratio after estrogen withdrawal (related to main Figure 1). Gene expression analysis of dickkopf-1 (*Dkk1*), lymphoid enhancer-binding factor 1 (*Lef1*), axin-related protein 2 (*Axin2*), receptor Activator of NF-κB Ligand (*Rankl*), and osteoprotegerin (*Opg*) in femoral bone tissue of Sham vs. OVX operated 14-week-old *Dkk1$^{fl/fl}$;Rosa26-CreERT2* and control mice was performed using Real-time PCR. Cre- Sham, n = 12; Cre- OVX, n = 12; Cre+ Sham, n = 10; Cre+ OVX, n = 12. Gene expression levels were normalized to *β-Actin.* Data represent the mean ± SD, Statistical analysis was performed using Two-way-ANOVA. *p<0.05, **p<0.01, ***p<0.001 vs. Sham or #p<0.05, ##p<0.01, ###p<0.001 vs. respective Cre-negative control.

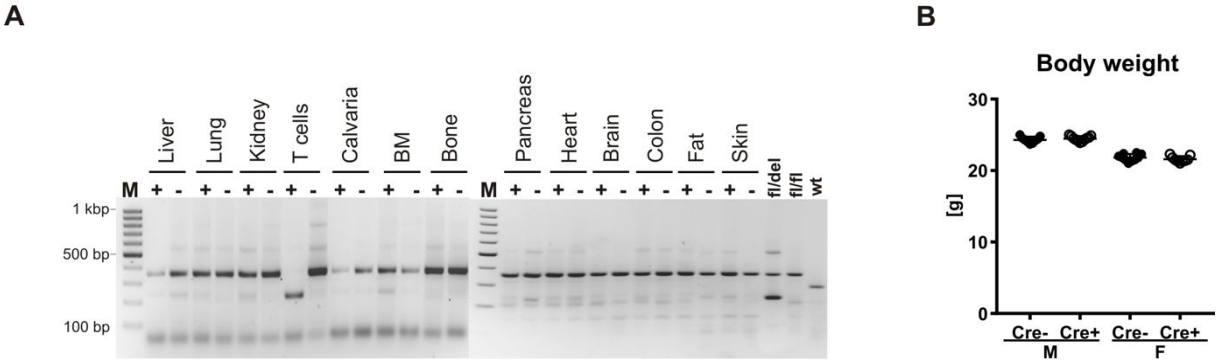

Figure S2. ***Dkk1$^{fl/fl}$;Lck-Cre*** **mice exhibit T cell-specific *Dkk1* deletion (related to main Figure 3).** (A) Recombinatory efficiency of Lck-Cre was analyzed. Representative examples of tissue-specific Cre recombination analyzed by PCR of *Dkk1$^{fl/fl}$;Lck-Cre* and control mice. Controls represent *Dkk1* deletion (fl/del: 228bp), floxed *Dkk*1 (fl/fl: 358bp), and wild-type (wt: 288 bp). (B) Body weight of *Dkk1$^{fl/fl}$;Lck-Cre* and control mice was determined. Statistical analysis was performed by the Student's t-test.

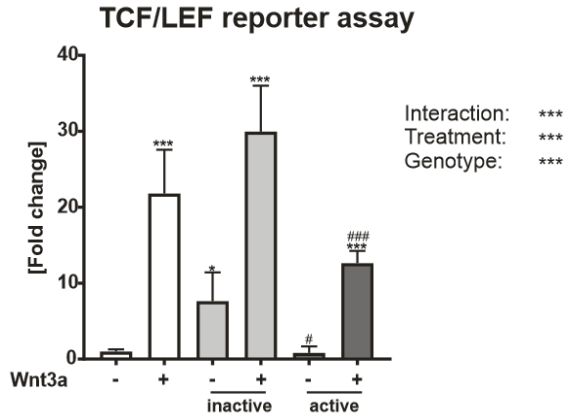

Figure S3. **CM from activated T cells suppressed Wnt3a-induced TCF/LEF Wnt promoter activity (related to main Figure 5).** TCF/LEF reporter assay of C2C12 cells treated with CM from activated or inactivated T cells for 48h. n = 6 biological replicates per group. Data represent the mean ± SD. Statistical analysis was performed by the Two-Way-ANOVA *p<0.05, **p<0.01, ***p<0.01 vs. untreated or #p<0.05, ##p<0.01, ###p<0.001 vs. respective inactive control.

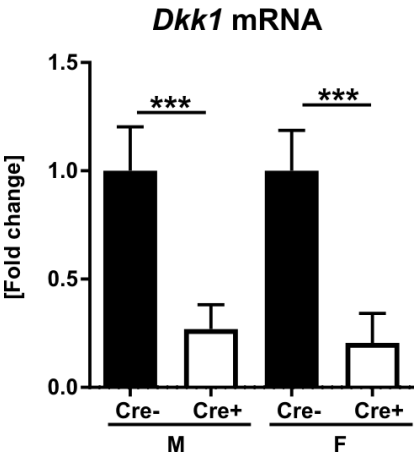

Figure S4. Global *Dkk1* deletion successfully reduced *Dkk1* expression in T cells (related to main Figure 5). *Dkk1* mRNA expression in T cells of 12-week old *Dkk1*$^{fl/fl}$*;Lck-Cre* and Cre-negative control mice was analyzed using Real-time PCR. n = 8 animals group. Gene expression levels were normalized to *β-Actin.* Data represent the mean ± SD. Statistical analysis was performed by the Student's *t*-test.*p<0.05, **p<0.01, ***p<0.001.

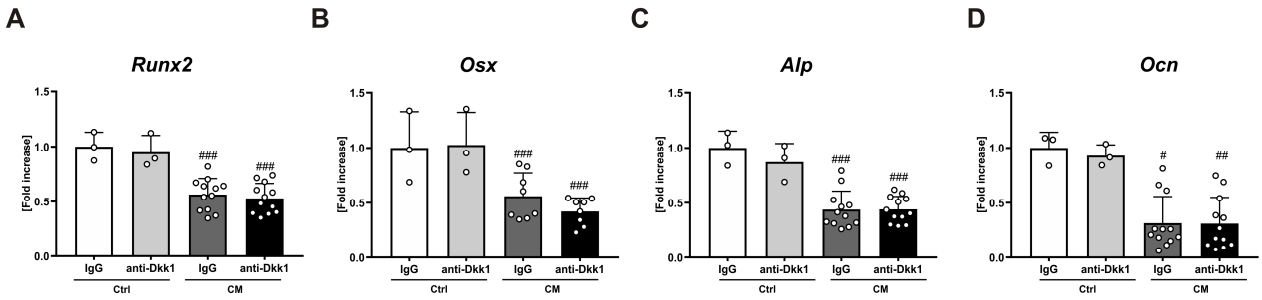

Figure S5. Neutralization of DKK1 does not restore the downregulation of osteoblastic marker genes (related to main Figure 5). Primary osteoblasts from 12-week-old wild-type mice were differentiated and treated with CM from activated WT T cells in the presence of a DKK1 antibody or an isotype control for 7 days. Gene expression analysis of the osteogenic genes (A) Runt-related transcription factor 2 (*Runx2*), (B) osterix (*Osx*), (C) alkaline phosphatase (*Alp*), and (D) and osteocalcin (*Ocn*) was performed using real-time PCR. Gene expression levels were normalized to *β-Actin.* Data represent the mean ± SD. n = 3 individual mice per group (plus combinations of T cell CM from up to 4 individual mice). Statistical analysis was performed using Two-way-ANOVA. *p<0.05, **p<0.01, ***p<0.01 vs. inactive or #p<0.05, ##p<0.01, ###p<0.001 vs. respective isotype control.

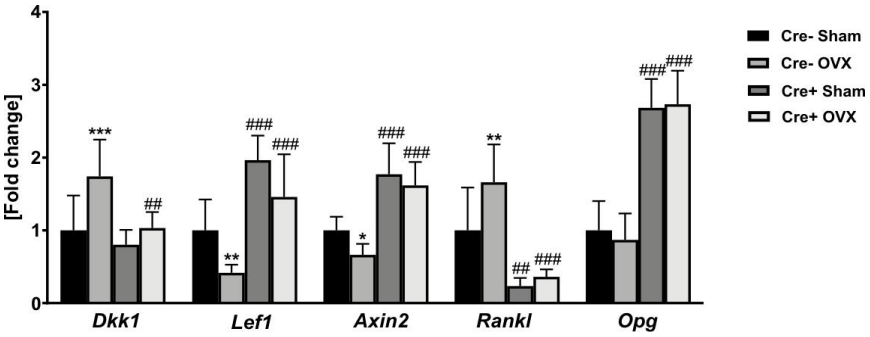

Figure S6. T cell-specific *Dkk1* cKO mice exhibit altered Wnt signaling as well as *Rankl/Opg* ratio after estrogen withdrawal (related to main Figure 6). Gene expression analysis of dickkopf-1 (*Dkk1*), lymphoid enhancer-binding factor 1 (*Lef1*), axin-related protein 2 (*Axin2*), receptor Activator of NF-κB Ligand (*Rankl*), and osteoprotegerin (*Opg*) in femoral bone tissue of Sham vs. OVX operated 14-week-old *Dkk1$^{fl/fl}$;Lck-Cre* and control mice was performed using Real-time PCR. Cre- Sham, n = 8; Cre- OVX, n = 11; Cre+ Sham, n = 9; Cre+ OVX, n = 10. Gene expression levels were normalized to *β-Actin.* Data represent the mean ± SD, Statistical analysis was performed using Two-way-ANOVA. *p<0.05, **p<0.01, ***p<0.001 vs. Sham or #p<0.05, ##p<0.01, ###p<0.001 vs. respective Cre-negative control.

Supplementary Table 1 (related to main Figure 2). Total number (*10^6) of splenic T cell populations and bone marrow-derived myeloid suppressor cells and spleen-derived B cells in sham vs. ovariectomized (OVX) *Dkk1$^{fl/fl}$;Rosa26-CreERT2*, *Dkk1$^{fl/fl}$;Osx-Cre* and *Dkk1$^{fl/fl}$;Dmp1-Cre* mice and their respective controls.

		Cre-			Cre+	
Cell populations	**Sham**	**OVX**	**P value and % change**	**Sham**	**OVX**	**P value and % change**
Dkk1$^{fl/fl}$;Rosa26-CreERT2	**n=13**	**n=15**		**n=13**	**n=10**	
$CD3^+$	17.2 ± 1.32	21.9 ± 3.42	<0.05 +27%	19.7 ± 3.85	23.4 ± 2.18	<0.05 +19%
$CD11b^+GR1^+$	1.75 ± 0.41	1.65 ± 0.25	>0.999 -6%	1.78 ± 0.39	1.79 ± 0.43	>0.999 +1%
$CD45R^+$	36.0 ± 5.43	38.2 ± 4.55	0.954 +6%	33.7 ± 6.75	36.4 ± 6.02	0.898 +8%
Dkk1$^{fl/fl}$;Osx-Cre	**n=13**	**n=15**		**n=13**	**n=10**	
$CD3^+$	11.7 ± 2.54	15.3 ± 2.56	<0.05 +31%	11.6 ± 2.34	14.7 ± 1.69	<0.05 +27%
$CD3^+CD4^+$	4.24 ± 0.68	5.80 ± 1.00	<0.05 +37%	4.64 ± 1.08	5.95 ± 0.85	<0.05 +28%
$CD3^+CD4^+CD69^+$	0.38 ± 0.07	0.52 ± 0.08	<0.001 +37%	0.45 ± 0.05	0.55 ± 0.05	<0.01 +22%
$CD3^+CD8^+$	4.40 ± 0.68	5.57 ± 0.89	<0.05 +27%	4.58 ± 0.69	5.75 ± 0.98	<0.05 +26%
$CD3^+CD8^+CD69^+$	0.13 ± 0.03	0.18 ± 0.04	<0.05 +38%	0.13 ± 0.02	0.18 ± 0.03	<0.05 +38%
$CD11b^+GR1^+$	1.69 ± 0.24	1.73 ± 0.25	>0.999 +2%	1.77 ± 0.18	1.80 ± 0.20	>0.999 +2%
$CD45R^+$	30.0 ± 6.84	30.9 ± 4.98	>0.999 +3%	30.7 ± 6.40	31.3 ± 4.36	>0.999 +2%
Dkk1$^{fl/fl}$;Dmp1-Cre	**n=13**	**n=15**		**n=13**	**n=10**	
$CD3^+$	12. ± 2.39	15.4 ± 1.31	<0.05 +19%	13.0 ± 2.18	15.7 ± 1.95	<0.05 +21%
$CD3^+CD4^+$	4.11 ± 0.80	5.12 ± 0.76	<0.05 +25%	3.95 ± 0.65	5.01 ± 0.99	<0.05 +27%
$CD3^+CD4^+CD69^+$	0.52 ± 0.09	0.73 ± 0.18	<0.01 +40%	0.52 ± 0.06	0.72 ± 0.15	<0.01 +38%
$CD3^+CD8^+$	3.96 ± 0.65	4.76 ± 0.58	<0.05 +20%	3.66 ± 0.72	4.53 ± 0.62	<0.05 +24%
$CD3^+CD8^+CD69^+$	0.12 ± 0.02	0.15 ± 0.02	<0.05 +25%	0.13 ± 0.02	0.16 ± 0.02	<0.05 +23%
$CD11b^+GR1^+$	1.38 ± 0.39	1.42 ± 0.18	>0.999 +3%	1.45 ± 0.36	1.51 ± 0.30	0.999 +4%
$CD45R^+$	31.2 ± 4.99	31.6 ± 3.25	>0.999 +1%	31.8 ± 3.17	31.9 ± 3.76	>0.999 +0%

Cell types were distinguished by flow cytometry according to the indicated surface markers. $CD3^+$ = T cells, $CD3^+CD4^+$ = T helper cells, $CD3^+CD4^+CD69^+$ = activated T helper cells, $CD3^+CD8^+$ = cytotoxic T cells, $CD3^+CD8^+CD69^+$ = activated cytotoxic T cells, $CD11b^+GR1^+$ = myeloid-derived suppressor cells, $CD45R^+$ = B cells. Data represent the mean ± SD. Statistical analysis was performed by the Two-Way-ANOVA. #p<0.05, ##p<0.01, ###p<0.001 vs respective Cre negative control.

Supplementary Table 2 (related to main Figure 3). Bone microstructure and histological parameters of the femora and tibiae of 12-week-old *Dkk1$^{fl/fl}$;Lck-Cre* mice.

	Male			Female		
	Cre- (n=9)	**Cre+ (n=11)**	***P* value and % change**	**Cre- (n=9)**	**Cre+ (n=8)**	***P* value and % change**
Dkk1$^{fl/fl}$;Lck-Cre	**n=9**	**n=11**		**n=9**	**n=8**	
*µCT**						
BV/TV [%]	7.76 ± 0.51	10.5 ± 0.43	<0.001 +35%	1.17 ± 0.80	2.02 ± 0.83	<0.05 71%
Tb.N [1/mm]	4.21 ± 0.33	4.75 ± 0.53	<0.05 +13%	2.31 ± 0.45	2.83 ± 0.17	<0.01 23%
Tb.Th [µm]	41. 1 ± 5.16	43.2 ± 3.64	0.306 +5%	33.4 ± 2.07	36.6 ± 3.86	0.051 10%
Tb.Sp [mm]	0.24 ± 0.02	0.22 ± 0.03	<0.05 -8%	0.40 ± 0.06	0.35 ± 0.03	<0.05 -13%
Histomorphometry#						
MS/BS [%]	21.0 ± 2.45	22.9 ± 2.51	0.125 +9%	26.0 ± 3.40	28.4 ± 2.06	0.095 +9%
MAR [µm/d]	1.72 ± 0.35	2.27 ± 0.56	<0.05 +32%	1.77 ± 0.58	2.51 ± 0.79	<0.05 42%
BFR/BS [$\mu m^3/\mu m^2/d$]	0.33 ± 0.16	0.52 ± 0.13	<0.01 +58%	0.48 ± 0.22	0.73 ± 0.16	<0.05 52%
N.Ob/B.Pm [#/mm]	26.5 ± 5.66	29.1 ± 6.27	0.352 +10%	18.9 ± 3.83	19.6 ± 3.09	0.697 +4%
N.Oc/B.Pm [#/mm]	4.27 ± 1.41	2.85 ± 1.07	<0.05 -33%	6.28 ± 1.24	4.15 ± 1.12	<0.01 -34%

BV/TV = bone volume/total volume, Tb.N = trabecular number, Tb.Th = trabecular thickness, Tb.Sp = trabecular separation, MS/BS = mineralizing surface/bone surface, MAR = mineral apposition rate, BFR/BS = bone formation rate/bone surface, N.Ob/B.Pm = number of osteoblasts, N.Oc/B.Pm = number of osteoclasts/bone perimeter. Data represent the mean ± SD. Statistical analysis was performed by the Student's t-test.*p<0.05, **p<0.01, ***p<0.001 vs. Cre-negative control. *µCT was performed at the femur. #undecalficied histology for bone formation parameters was determined at the tibia. Number of osteoblasts and osteoclasts was determined at the femur.

Supplementary Table 3 (related to main Figure 1 and 3). Total number of splenic and thymic T cell populations in *Dkk1$^{fl/fl}$;Rosa26-CreERT2 and Dkk1$^{fl/fl}$;Lck-Cre* mice and their respective controls.

Cell populations	Cre-	Cre+	P value
Dkk1$^{fl/fl}$;Rosa26-CreERT2 Spleen	**n=3**	**n=3**	
Total counts (*10^6)	19.4 ± 2.90	23.1 ± 7.32	0.463 +19%
$CD3^+CD4^+$	2.57 ± 0 .43	3.49 ± 1.40	0.338 +26%
$CD3^+CD4^+CD69^+$	0.30 ± 0.07	0.36 ± 0.09	0.478 +20%
$CD3^+CD8^+$	2.33 ± 0.41	3.02 ± 0.87	0.107 +30%
$CD3^+CD8^+CD69^+$	0.04 ± 0.01	0.05 ± 0.02	0.469 +25%
$CD4^+CD25^+FoxP_3^+$	0.26 ± 0.03	0.33 ± 0.14	0.441 27%
$CD4^+TCR\beta^+CD44^{low}CD62L^{high}$	0.23 ± 0.17	0.19 ± 0.13	0.651 -17%
Dkk1$^{fl/fl}$;Rosa26-CreERT2 Thymus	**n=3**	**n=3**	
Total counts (*10^6)	65.3 ± 13.4	44.1 ± 15.3	0.145 -32%
$CD4^+CD8^+$	53.8 ± 11.5	36.9 ± 12.8	0.164 -31%
$CD4^+$	3.42 ± 0.51	2.07 ± 0.73	0.058 -39%
$CD8^+$	1.15 ± 0.46	0.47 ± 0.09	0.064 -59%
$CD4^-CD8^-$	2.60 ± 0.46	1.22 ± 0.39	$0.017^{\#}$ -53%
***Dkk1$^{fl/fl}$;Lck-Cre* Spleen**	**n=5**	**n=3**	
Total counts (*10^6)	22.0 ± 11.2	24.3 ± 6.35	0.756 +10%
$CD3^+CD4^+$	2.67 ± 1.53	2.96 ± 0.80	0.755 +11%
$CD3^+CD4^+CD69^+$	0.17 ± 0.09	0.19 ± 0.08	0.727 +12%
$CD3^+CD8^+$	2.12 ± 1.02	2.39 ± 0.58	0.696 +13%
$CD3^+CD8^+CD69^+$	0.06 ± 0.03	0.07 ± 0.03	0.766 +17%
$CD4^+CD25^+FoxP_3^+$	0.28 ± 0.16	0.17 ± 0.03	0.301 -39%
$CD4^+TCR\beta^+CD44^{low}CD62L^{high}$	0.32 ± 0.16	0.29 ± 0.08	0.755 -9%
***Dkk1$^{fl/fl}$;Lck-Cre* Thymus**	**n=5**	**n=3**	
Total counts (*10^6)	65.3 ± 27.3	100 ± 57.2	0.278 +53%
$CD4^+CD8^+$	43.9 ± 18.1	66.5 ± 37.2	0.281 +51%
$CD4^+$	2.44 ± 1.43	5.22 ± 3.06	0.123 +114%
$CD8^+$	0.98 ± 0.79	1.77 ± 1.06	0.275 +81%
$CD4^-CD8^-$	1.10 ± 0.53	2.11 ± 1.18	0.135 +92%

Cell types were distinguished by flow cytometry according to the surface markers. Data represent the mean ± SD. Statistical analysis was performed by student`s *t*-test. #p<0.05.

Supplementary Table 4 (related to main Figure 6). Bone phenotype of third and fourth vertebral body from 14-week-old female sham vs. ovariectomized (OVX) *Dkk1$^{fl/fl}$;Lck-Cre* mice.

		Cre-			*Cre+*	
Spine	**Sham**	**OVX**	**P value and % change**	**Sham**	**OVX**	**P value and % change**
Dkk1$^{fl/fl}$;Lck-Cre	**n=9**	**n=12**		**n=9**	**n=11**	
µCT						
Tb.N [1/mm]	3.53 ± 0.25	3.14 ± 0.32	<0.05 -12%	3.96 ± 0.26$^{\#}$	3.62 ± 0.44$^{\#\#}$	0.095 -9%
Tb.Sp [mm]	0.30 ± 0.03	0.34 ± 0.03	<0.05 +8%	0.26 ± 0.02$^{\#}$	0.26 ± 0.03$^{\#\#\#}$	>0.999 +0%
Histomorphometry						
MS/BS [%]	23.7 ± 3.07	25.5 ± 3.07	>0.999 +8%	25.4 ± 2.10	26.2 ± 3.57	>0.999 +3%
MAR [µm/d]	1.63 ± 0.29	2.56 ± 0.69	<0.01 +57%	2.50 ± 0.34$^{\#}$	2.58 ± 0.57	0.406 +3%
N.Ob/B.Pm [#/mm]	18.4 ± 3.47	19.0 ± 3.97	>0.999 +3%	19.2 ± 2.87	21.2 ± 2.61	>0.999 +10%

MAR = mineral apposition rate, BFR/BS = bone formation rate/bone surface, N.Ob/B.Pm = number of osteoblasts, N.Oc/B.Pm = number of osteoclasts/bone perimeter. Data represent the mean ± SD. Statistical analysis was performed by the Two-Way-ANOVA. #p<0.05, ##p<0.01, ###p<0.001 vs respective Cre negative control.

Supplementary Table 5 (related to main Figure 6). Total number [*10^6] of splenic T cells populations and bone marrow-derived myeloid suppressor cells and spleen-derived B cells in sham operated vs. ovariectomized (OVX) *Dkk1$^{fl/fl}$;Lck-Cre* mice.

		Cre-			**Cre+**	
Cell populations	**Sham (n=6)**	**OVX (n=6)**	***P* value and % change**	**Sham (n=6)**	**OVX (n=6)**	***P* value and % change**
Dkk1$^{fl/fl}$;Lck-Cre	**n=6**	**n=6**		**n=6**	**n=6**	
$CD3^+$	21.0 ± 2.79	26.0 ± 2.14	<0.001 +24%	20.0 ± 2.71	24.3 ± 1.22	<0.05 +21%
$CD3^+CD4^+$	5.51 ± 0.73	6.99 ± 0.77	<0.05 +27%	5.65 ± 0.74	6.63 ± 0.67	0.177 +17%
$CD3^+CD4^+CD69^+$	0.72 ± 0.10	1.02 ± 0.12	<0.001 +42%	0.71 ± 0.06	0.93 ± 0.15	<0.05 +31%
$CD3^+CD8^+$	5.13 ± 0.79	6.23 ± 0.52	<0.05 +18%	5.13 ± 0.57	6.11 ± 0.53	0.071 +19%
$CD3^+CD8^+CD69^+$	0.16 ± 0.03	0.20 ± 0.03	<0.05 +22%	0.16 ± 0.02	0.18 ± 0.03	>0.999 +13%
$CD11b^+GR1^+$	1.93 ± 0.51	1.95 ± 0.15	>0.999 +1%	2.03 ± 0.28	1.95 ± 0.30	>0.999 -4%
$CD45R^+$	37.1 ± 7.05	40.0 ± 3.75	>0.999 +8%	36.8 ± 6.77	40.8 ± 5.75	>0.999 +11%

Cell types were distinguished by flow cytometry according to the indicated surface markers. $CD3^+$ = T cells, $CD3^+CD4^+$ = T helper cells, $CD3^+CD4^+CD69^+$ = activated T helper cells, $CD3^+CD8^+$ = cytotoxic T cells, $CD3^+CD8^+CD69^+$ = activated cytotoxic T cells, $CD11b^+GR1^+$ = myeloid-derived suppressor cells, $CD45R^+$ = B cells. Data represent the mean ± SD. Statistical analysis was performed by the Two-Way-ANOVA. #p<0.05, ##p<0.01, ###p<0.001 vs respective Cre negative control.

References

Baschant, U., Frappart, L., Rauchhaus, U., Bruns, L., Reichardt, H.M., Kamradt, T., Brauer, R., and Tuckermann, J.P. (2011). Glucocorticoid therapy of antigen-induced arthritis depends on the dimerized glucocorticoid receptor in T cells. Proc. Natl. Acad. Sci. *108*, 19317–19322.

Colditz, J., Thiele, S., Baschant, U., Niehrs, C., Bonewald, L.F., Hofbauer, L.C., and Rauner, M. (2018). Postnatal skeletal deletion of Dickkopf-1 increases bone formation and bone volume in male and female mice, despite increased sclerostin expression. J. Bone Miner. Res. *33*, 1698–1707.

Dempster, D.W., Compston, J.E., Drezner, M.K., Glorieux, F.H., Kanis, J.A., Malluche, H., Meunier, P.J., Ott, S.M., Recker, R.R., and Parfitt, A.M. (2013). Standardized nomenclature, symbols, and units for bone histomorphometry: a 2012 update of the report of the ASBMR Histomorphometry Nomenclature Committee. J. Bone Miner. Res. *28*, 2–17.

Pietilä, I., Ellwanger, K., Railo, A., Jokela, T., Barrantes, I. del B., Shan, J., Niehrs, C., and Vainio, S.J. (2011). Secreted Wnt antagonist Dickkopf-1 controls kidney papilla development coordinated by Wnt-7b signalling. Dev. Biol. *353*, 50–60.

Rauner, M., Franke, K., Murray, M., Singh, R.P., Hiram-Bab, S., Platzbecker, U., Chavakis, T., Hofbauer, L.C., and Wielockx, B. Increased EPO Levels Are Associated With Bone Loss in Mice Lacking PHD2 in EPO-Producing Cells; Increased EPO Levels Are Associated With Bone Loss in Mice Lacking PHD2 in EPO-Producing Cells.